Cerebral Cortex, 2017; 1–20

doi: 10.1093/cercor/bhx279
Original Article

ORIGINAL ARTICLE

Representations of Fine Digit Movements in Posterior and Anterior Parietal Cortex Revealed Using Long-Train Intracortical Microstimulation in Macaque Monkeys

Mary K. L. Baldwin[1], Dylan F. Cooke[1,2], Adam B. Goldring[1] and Leah Krubitzer[1,3]

[1]Center for Neuroscience, University of California, 1544 Newton Court, Davis, CA 95618, USA, [2]Department of Biomedical Physiology and Kinesiology, Simon Fraser University, 8888 University Drive, Burnaby, British Columbia, Canada V5A 1S6 and [3]Department of Psychology, University of California, Davis, CA 95618, USA

Address correspondence to Leah A. Krubitzer, Center for Neuroscience, University of California, 1544 Newton Court, Davis, CA 95618, USA.
E-mail: lakrubitzer@ucdavis.edu

Abstract

The current investigation in macaque monkeys utilized long-train intracortical microstimulation to determine the extent of cortex from which movements could be evoked. Not only were movements evoked from motor areas (PMC and M1), but they were also evoked from posterior parietal (5, 7a, 7b) and anterior parietal areas (3b, 1, 2). Large representations of digit movements involving only the index finger (D2) and thumb (D1), were elicited from areas 1, 2, 7b, and M1. Other movements evoked from these regions were similar to ethologically relevant movements that have been described in other primates. These include combined forelimb and mouth movements and full hand grasps. However, many other movements were much more complex and could not be categorized into any of the previously described ethological categories. Movements involving specific digits, which mimic precision grips, are unique to macaques and have not been described in New World or prosimian primates. We propose that these multiple and expanded motor representations of the digits co-evolved with the emergence of the opposable thumb and alterations in grip type in some anthropoid lineages.

Key words: grasping, posterior parietal cortex, primate, reaching, somatosensory cortex

Introduction

Since the advent of cortical stimulation studies, the full extent of "excitable cortex", or cortex in which movements can be evoked when electrically stimulated, has been contentious. In early studies using surface stimulation methods, differences in stimulation parameters resulted in vastly different motor maps. Longer duration stimulation evoked movements involving multiple joints or body parts while shorter durations resulted in maps of muscle "twitches" restricted to single joints and body parts (Taylor and Gross 2003). Further, long duration stimulation produced motor maps that extended over a large portion of the cortical surface, including both frontal and parietal cortical areas (Ferrier 1874), whereas shorter duration stimulation generated maps mostly restricted to cortex anterior to the central sulcus (Leyton and Sherrington 1917). Because of these differences in the types of movements evoked and the extent of motor maps generated with different electrical stimulation parameters, there was a heated debate at the turn of the

© The Author 2017. Published by Oxford University Press. All rights reserved. For Permissions, please e-mail: journals.permissions@oup.com

Downloaded from https://academic.oup.com/cercor/advance-article-abstract/doi/10.1093/cercor/bhx279/4608060
by University of California, Davis user
on 26 March 2018

20th century over whether cortex on the precentral and postcentral gyrus of primates should be collectively called sensorimotor cortex or should instead be considered separate sensory and motor cortical fields (Penfield and Boldrey 1937; Taylor and Gross 2003).

With the advent of intracortical microelectrode stimulation techniques (ICMS) in the late 1960s and early 1970s, most investigators moved towards using short-train stimulation (ST-ICMS). The goal was to identify cortical neuron clusters that directly project to motoneuron pools in the spinal cord that control the forearm (Stoney et al. 1968), and to reveal the topographic organization of this cortical efferent system (Asanuma and Rosen 1972). The use of ST-ICMS was ubiquitous in subsequent decades, despite the fact that the temporal characteristics of ST-ICMS (e.g., 20–50 ms) are often only a 10th of the duration it takes for natural movements to occur (e.g., 200 ms to several seconds). Thus, the goal of ICMS studies was to elicit barely detectable single muscle twitches by applying the least amount of current at short durations. One prominent thought at the time was that motor cortex represented movements of single muscles in a topographic manner (e.g. McGuinness et al. 1980). However, systematic studies using ST-ICMS techniques revealed that motor cortex was organized in a mosaic fashion, with the same muscles or movements represented at multiple different locations separated by representations of other body parts that were not always somatotopically adjacent (i.e., digit representations were adjacent to that of the shoulder) (Gould et al. 1986; Preuss et al. 1996; Kambi et al. 2011). Further, findings from spike-triggered averaging studies showed that there was not a one-to-one correspondence between the firing pattern of a single neuron in M1 and a single muscle (Fetz and Cheney 1980); rather a single neuron could have facilitative or suppressive effects on multiple muscles and often had such effects on both agonist and antagonist muscle groups (Kasser and Cheney 1985).

In the beginning of this century, long-train stimulation techniques (LT-ICMS) were introduced by Graziano et al. (2002a) to approximate the duration of a natural reach movement of a monkey (500 ms). Rather than the small twitches evoked using ST-ICMS, these investigators evoked complex movements of multiple joints (e.g., hand-to-mouth, hand postures around the body). Using these stimulation parameters, they suggest that one of the organizing principles of motor cortex is the representation of ethologically relevant behaviors that form action maps (Graziano 2016). The use of LT-ICMS, however, has been controversial, with many studies suggesting that the resulting complex movements are due to "spread of current" (Strick 2002), or that this method "highjacks" the system in awake animals, and thus does not represent natural motor output within the motor network (Griffin et al. 2011; see Discussion). Regardless of these arguments, LT-ICMS has proven to be a powerful tool in anesthetized animals for elucidating and comparing the organization of movement representations in motor and premotor cortex in a variety of primates (Graziano et al. 2002a; Stepniewska et al. 2005; Stepniewska et al. 2009b; Gharbawie et al. 2011a, 2011b), closely related mammals such as tree shrews (Baldwin et al. 2017), and other mammals such as rats (Bonazzi et al. 2013; Brown and Teskey 2014).

Like the original findings by Graziano and colleagues, the types of movements evoked using LT-ICMS in motor cortex of other species have often been categorized into distinct complex movement types involving multiple joints or body parts such as grasping, reaching, and hand-to-mouth. Further, studies utilizing LT-ICMS have demonstrated that movements can be evoked from posterior parietal cortex (PPC) in primates (Kaas et al. 2017) and even somatosensory cortex in tree shrews (Baldwin et al. 2017). Interestingly, while the original studies using LT-ICMS were made in macaque monkeys, to date only a few studies have used LT-ICMS to explore movement representations in cortex posterior to the central sulcus of macaque monkeys. These studies revealed domains specific for eye movements (LIP: (Thier and Andersen 1998)), defensive movements (VIP: (Cooke et al. 2003)), and grasping movements (area 2: (Gharbawie et al. 2011b); area 5: (Rathelot et al. 2017)) (Fig. 1). However, only limited portions of anterior parietal cortex and PPC have been explored in macaque monkeys (Fig. 1), and it is

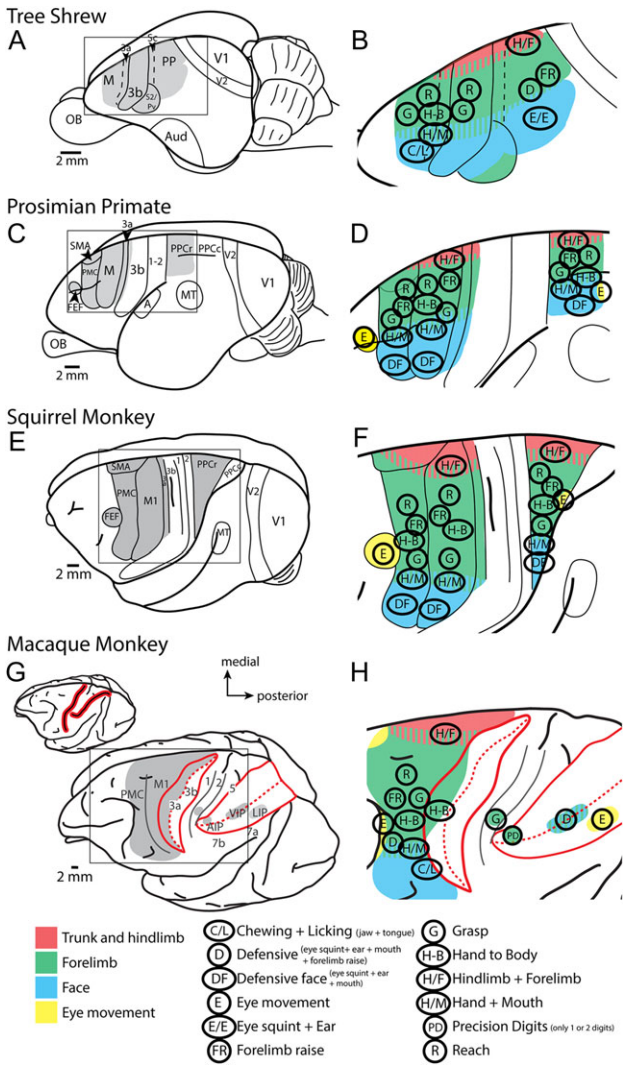

Figure 1. Comparative summary of previous LT-ICMS studies. Schematic organization of motor representations determined using LT-ICMS in different primates and tree shrews. (*A*, *C*, *E*, *G*) Depict the areas of the cortex that were explored utilizing LT-ICMS (shaded gray). (*B*, *D*, *F*, *H*) An enlarged view of these areas with different ethologically relevant movement domains encircled (see key at the bottom of the figure). These figures also demonstrate the general topographic organization of motor representations (see color key at bottom of the figure). Anatomical borders are indicated by solid or dashed lines. The red lines in (*G*) indicate the location of the intraparietal and central sulci in macaque monkeys (closed in inset at top) opened in expanded view. The key at the bottom left denotes specific movement types that have been described. Prior to the current study, macaque parietal cortex has not been widely explored using LT-ICMS. Data are redrawn from Baldwin et al. 2017; Stepniewska et al. 2005; Kaas et al. 2017; Graziano et al. 2002a, b; Cooke et al. 2003, Thier and Andersen 1998, Gharbawie et al. 2011a, 2011b; Rathelot et al. 2017. Areas 3a, 3b, and 1 had not been explored. See Table 1 for abbreviations.

Downloaded from https://academic.oup.com/cercor/advance-article-abstract/doi/10.1093/cercor/bhx279/4608060
by University of California, Davis user
on 26 March 2018

unknown if movements can be elicited from more than these restricted regions in anterior parietal cortex and PPC.

In the current study we utilized LT-ICMS techniques to explore motor, anterior parietal, and PPC in anesthetized macaque monkeys to address 3 goals. The first goal was to determine the extent of cortex from which movements could be evoked. The second was to determine if some of the features of motor maps (e.g., movement type) could be directly related to individual, anatomically defined cortical fields, or if there are other organizational principles that are not restricted to anatomical demarcations. Finally, from an evolutionary perspective, we hoped to determine if movement representations in parietal cortex are composed of similar ethologically relevant domains that have been described in New World and prosimian primates, or if the representations are more nuanced and serve as general-purpose modules that could be combined to produce a more flexible manual repertoire (Table 3).

Materials and Methods

The organization of motor maps was examined using long-train intracortical microstimulation (LT-ICMS) in 6 adult macaque monkeys (2 males and 4 females) ranging between 4 and 14 years of age weighing between 5.3 and 9.6 kg (Table 2). All surgical procedures were approved by the UC Davis IACUC, and followed NIH guidelines.

Surgical Procedures

Animals were initially anesthetized with an intramuscular injection of ketamine (20–30 mg/kg) and subsequent surgical procedures were carried out under isoflurane anesthesia (2%).

Table 1 List of abbreviations

1	Area 1
2	Area 2
3a	Area 3a
3b	Area 3b/primary somatosensory cortex
5	Area 5
7a	Area 7a
7b	Area 7b
AS	Arcuate sulcus
CS	Central sulcus
IPS	Intraparietal sulcus
LT-ICMS	Long-train intracortical microstimulation
M1	Primary motor cortex
PMC	Premotor cortex
PMCd	Dorsal premotor cortex
PMCv	Ventral premotor cortex
PPC	Posterior parietal cortex
ST-ICMS	Short-train intracortical microstimulation

Following surgery, animals were maintained under anesthesia using intravenous administration of ketamine (25–35 mg/kg/h), and supplemental intramuscular injections of xylazine (1 mg/kg). Heart rate, respiration rate, SPO_2 levels, body temperature, muscle tone, and reflexes were monitored throughout the experiment in order to ensure a constant level of anesthesia.

Once anesthetized, animals were intubated, cannulated, and catheterized. Subcutaneous injections of lidocaine (2%) were placed at the ears and topical lidocaine was applied to the external ear canals. Animals were then placed in a stereotax and positioned such that their upper trunk and forelimbs were unobstructed. Ophthalmic ointment was placed in the eyes to prevent drying. Subcutaneous injections of lidocaine (2%) were made at the midline of the scalp prior to making a surgical incision to expose the skull. Atropine (0.04 mg/kg) and dexamethasone (1 mg/kg) were administered. The scalp was cut, the temporal muscles were retracted, and a craniotomy was made to expose portions of frontal and parietal cortex. Once the dura was removed, liquid silicone was placed over the cortex to prevent desiccation, and a photograph of the cortical surface was imaged and printed so that stimulation site locations could be recorded relative to cortical vascular patterns and sulcal landmarks (Fig. 2).

ICMS Motor Mapping

Stimulation pulses were generated using a Grass S88 stimulator and two SIU stimulus isolation units and delivered using a low impedance (around 0.1 MΩ) microelectrode. Stimulation amplitude, duration, and frequency were measured by the voltage drop across a 10-kΩ resistor in series with the return lead of the stimulation isolation units. An LED positioned in the video frame was connected to the stimulator so that it was illuminated during the stimulation train. Electrical stimulation consisted of 500-ms trains of biphasic pulses (each phase 0.2 ms in duration) delivered at 200 Hz.

The stimulation electrode was lowered into the cortex using a micromanipulator to a depth of 1800 μm, which corresponds to the depth of cortical layers V and VI. For cortex within the sulci, the electrode was advanced parallel to the pial surface and stimulation was administered every 500 μm up to a maximum depth of 7.8 mm. An initial current amplitude of 50 μA was used, then increased if it was not strong enough to elicit a movement. If no movement was evoked for amplitudes of up to 600 μA, the site was considered to be nonexcitable. Threshold values were determined as the stimulus intensity for which an evoked movement could be elicited approximately 50% of the time, or a value (i.e., 17.5 μA) between an intensity that could evoke movements all of the time (20 μA), and an intensity for which no movements could be evoked (15 μA). To confirm the stability of anesthesia, and therefore our ability to

Table 2 Summary of cases and data

Case #	Sex	Age (years)	Hemisphere studied	Data collected		
				Motor stim	Somatosensory mapping	Figure
14–07	Female	13	Right	X	X	Table 3
14–117	Male	4	Left	X	–	Supplementary 1–4 and Table 3
14–132	Female	10	Left	X	X	Figs 6, 7, 9, and 11, Supplementary 4, and Table 3
15–57	Female	14	Left	X	–	Supplementary 1–4 and Table 3
15–74	Male	7	Left	X	–	Supplementary 1–4 and Table 3
15–84	Female	12	Left	X	–	Figs 2, 3, 4, 5, 7, and 8, Supplementary 4, and Table 3

Downloaded from https://academic.oup.com/cercor/advance-article-abstract/doi/10.1093/cercor/bhx279/4608060
by University of California, Davis user
on 26 March 2018

Table 3 Summary of sites tested across cortical areas

Body part included in evoked movement	PMC	M1	3b	1	2	5	7	Totals
Forelimb	20	215	30	63	69	26	112	535
Digits	3	95	16	46	55	25	84	324
Face	12	65	11	16	3	–	28	135
Hindlimb	2	25	–	–	–	–	–	27
Trunk/neck	2	28	–	–	–	–	–	30
Multiforelimb joints	6	135	17	16	26	4	47	251
Multiface	5	28	2	6	–	–	11	52
Forelimb + face	4	16	–	3	–	–	5	39
Forelimb + hind limb	2	8	–	–	–	–	–	10
Trunk or neck combinations	2	17	–	–	–	–	–	19
Elicited movement	30	300	41	76	74	26	131	678
No movement	4	13	0	65	61	42	129	314
Total sites tested	34	313	41	141	135	68	260	992

Forelimb includes shoulder, elbow, wrist, and digits.
Face includes eyebrow, eyelids, cheek, vibrissae, jaw, lips, and tongue.
Multiforelimb includes movements with 2 or more forelimb joints (i.e., wrist and digits).
Multiface includes movements with 2 or more facial components (i.e., jaw and tongue).
Trunk or neck combinations includes movements of the face, forelimb, and or hind limb movements that were combined with the trunk and/or neck.
Totals in right hand column are the sum across areas, but totals at the bottom cannot be reached by summing columns because of overlap. Numbers are based on results from 6 monkeys.

consistently evoke movements, throughout the experiment we periodically returned to stimulation sites within M1 to retest threshold values and movement parameters. Differences in threshold values across cortical areas and regions were tested using standard two-tailed unequal variance *t*-tests (Supplementary Fig. S4). A probability value of less than 0.05 was considered statistically significant.

All movements were digitally recorded from two angles (Sanyo Xacti VPC-HD2000A, 1920 × 1080 resolution, 60 frame/s) and analyzed offline (see Movement Analysis). Fiducial probes (fluorescent dyes) were placed at strategic locations within cortex to align functional and histological data.

Electrophysiological Recording

Receptive field (RF) location and stimulus preferences for neurons at some of the ICMS electrode penetration sites were obtained in two cases in areas 1 and 2 in order to compare the somatosensory RFs with evoked movements. All recordings were conducted at a depth of approximately 1000 μm from the cortical surface using the same electrode that was used for ICMS. In this way we could directly compare the neural responses and the evoked movement at the same site. Neuronal RF locations were first determined at 1000 μm and then the electrode was lowered to a depth of 1800 μm in order to test ICMS responses.

For those sites tested for somatosensory RF location, once the electrode was in place the body surface was stimulated and the RFs for neurons at that site were determined. We characterized a RF as "cutaneous" if neurons responded to light brushing of the skin or hair or light touch of the skin with a probe. A RF was characterized as "deep" if neurons responded to stimulation requiring more forceful taps to the skin, light pressure, or joint, limb, and digit manipulation (Padberg et al. 2009).

Histological Procedures

Once ICMS mapping was complete, animals were given a lethal dose of sodium pentobarbital intravenously, and perfused transcardially with saline, followed by either 2% or 4% paraformaldehyde, then 2% or 4% paraformaldehyde with 10% sucrose added (pH 7.3). The brains were removed and postfixed with 4% paraformaldehyde for 3 h to 3 days, and then placed in a 30% sucrose solution for 48–60 h.

In some cases, the brain was blocked to only include the region posterior to the arcuate sulcus, anterior to the lunate sulcus, and dorsal to the posterior inferior temporal sulcus (Fig. 2). In other cases, the entire hemisphere was sectioned. During horizontal sectioning, a camera (Nikon DSLR 5200) was positioned over the brain so that block-face images of every section could be taken. The tissue was sectioned horizontally at a thickness of 50–60 μm using a freezing microtome. Sections were divided into 5 series: 1 series was processed for Nissl, and the remaining series were directly mounted onto glass slides for fluorescent probe analysis, or saved for another study.

In one case (14–117), the cortex was separated from underlying structures and artificially flattened. Anatomical borders for this case were determined using tissue sections processed for myelin, or were approximated based on border locations in other cases (see below).

We did not distinguish between subdivisions of areas 7 or 5 that have been described elsewhere (Gregoriou et al. 2006; Seelke et al. 2012), but instead only describe the larger divisions of areas 7a, 7b, and 5, which were readily defined using our stains. Furthermore, although we appreciate that multiple cortical areas have been described within the intraparietal sulcus, IPS (e.g., AIP, VIP, and LIP), we did not distinguish them, but instead define area 5 as continuing from the surface of the medial bank of the IPS to the fundus, where it borders area 7. Because we took images of each block face during cutting, we could readily follow the depth and location of electrode penetration sites, including stimulation sites within the central and intraparietal sulcus (Figs 2*B* and 3). Therefore, we could accurately determine which bank and what layer was stimulated when electrode penetrations advanced deep within sulci (as was the case for the highlighted depth sites 3–7 in case 15–84; see Fig. 4).

Downloaded from https://academic.oup.com/cercor/advance-article-abstract/doi/10.1093/cercor/bhx279/4608060
by University of California, Davis user
on 26 March 2018

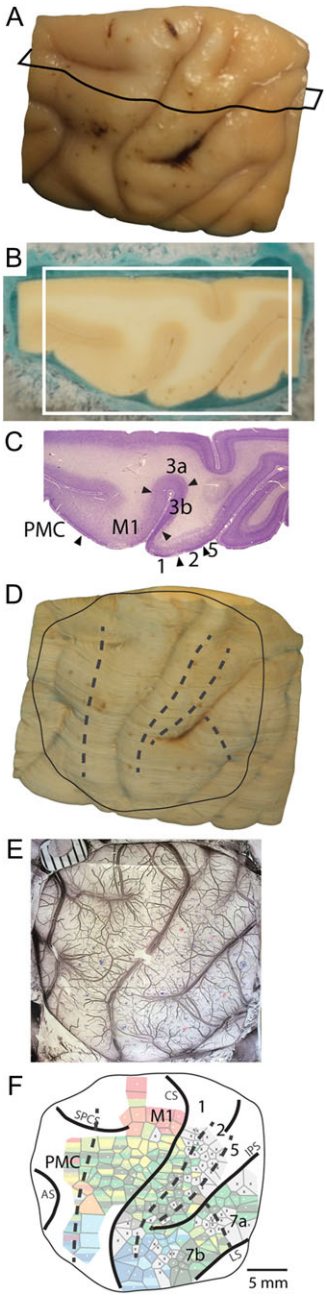

Figure 2. Alignment of anatomical borders and ICMS maps. After the completion of the ICMS mapping experiment, the brains were perfused, removed, and blocked (*A*). The brain was cryoprotected and then cut horizontally. During sectioning, an image was taken of the block-face prior to cutting each section (*B*). The black line in (*A*) represents the approximate location of the section presented in (*B*) within the block of tissue. Every fourth or fifth section was then processed for Nissl and borders of cortical fields were determined for each section in the series (*C*). The borders were then superimposed onto the corresponding block-face image for the section (alignment of Nissl falls within the white rectangle of (*B*)). All block-face images taken during sectioning with the borders superimposed were then imported into Fiji and a 3D reconstruction of the tissue block was recreated using the 3D view plug-in (*D*). This 3D reconstruction was then aligned with the photo taken during the ICMS mapping procedure on which electrode penetration sites were marked relative to vascular patterns (*E*). This procedure allowed us to accurately align anatomical borders to the reconstruction of our ICMS motor maps (*F*). Dashed lines in (*D*) and (*F*) mark architectonic boundaries. Rostral is to the left and medial is to the top. M1 = primary motor cortex; PMC = premotor cortex; somatosensory fields = 3b (S1), 1 and 2; posterior parietal fields = 5, 7a, 7b. CS is central sulcus, IPS is intraparietal sulcus, AS is arcuate sulcus, LS is lateral sulcus, and SPCS is superior precentral sulcus.

Physiological and Anatomical Alignment/ Reconstruction

Block-face images of all cortical sections were processed in Photoshop and were then imported into the Fiji processing package (Schindelin et al. 2012), and a 3D reconstruction was made using the 3D view plug-in. Locations of cortical field borders were superimposed on the individual horizontal images, which matched the sections that were processed for Nissl. Fiduciary probes were also indicated on their matching image. Electrode penetrations visible in tissue sections were also highlighted. These 3D reconstructions were then aligned to images of the surface of the brain using local landmarks such as sulcal locations, as well as electrode and fiducial probe penetration sites (Fig. 2*A*, *D*). This process allowed us to accurately align histologically determined cortical field boundaries to our microstimulation maps (Fig. 2*E*, *F*). Cortical borders for areas M1, 3a, 3b, 1, 2, 5, and 7b were determined with Nissl-stained sections (Fig. 2*C*), and were superimposed onto the block-face images for 3D reconstruction (Fig. 2*B*).

Photomicrographs (Microfire camera, Optronics, Goleta, CA, fitted to a Nikon E400 microscope, or captured on an Aperio ScanScope) of Nissl-stained sections were adjusted for brightness and contrast with Adobe Photoshop but were otherwise unaltered.

Movement Analysis and Motor Map Reconstruction

All movements were characterized by two independent observers, and were recorded during the experiment. These movements were later analyzed and confirmed offline. Movements were characterized by which joint or body part moved such as elbow, or tongue. When movements of multiple joints or body parts were observed, these were considered to be "complex" movements (Fig. 5). Further, because we were interested in specific digit movements associated with reaching and grasping behaviors we further defined digit movements based on the digits involved and whether the movements were flexions or extensions.

Representative movements were illustrated from frames captured just prior to stimulation initiation (baseline) and at the peak of the movement amplitude (apex). These frames were imported into Adobe Illustrator where the outline of the body movement was traced (Fig. 5). Although previous studies have evoked eye movements in a small portion of PPC (e.g., eye movements have been evoked from LIP; Their and Andersen 1998), we did not monitor eye movements in the current study.

ICMS-evoked movement displacement profiles were generated by importing the experimental recordings into Tracker analysis and modeling software (http://physlets.org/tracker/), and the position of a given body part was monitored and recorded for each frame (1/60 s) relative to ICMS stimulation onset and offset. A scale bar near the location of the moving body part served to calibrate the movement displacements during stimulation.

Voronoi tessellations in motor maps (Figs 4 and 6, and Supplementary Fig. S1) were created with an Adobe Illustrator script (https://github.com/fabianmoronzirfas/Illustrator-Javascript-Voronoi) based on the location of stimulation sites. The voronoi tessellation script is designed to create borders at equidistant locations between stimulation sites. Maps generated with this technique are similar to those previously used for illustrating motor representations in cortex (Nudo et al. 1992; Remple et al. 2006; Cooke et al. 2012; Baldwin et al. 2017) and have been used for sensory cortex as well (Kilgard and Merzenich 1998; Bao et al. 2001; De Villers-Sidani et al. 2007). This method is more precise than the hand drawn interpolation lines that have been traditionally used

Downloaded from https://academic.oup.com/cercor/advance-article-abstract/doi/10.1093/cercor/bhx279/4608060
by University of California, Davis user
on 26 March 2018

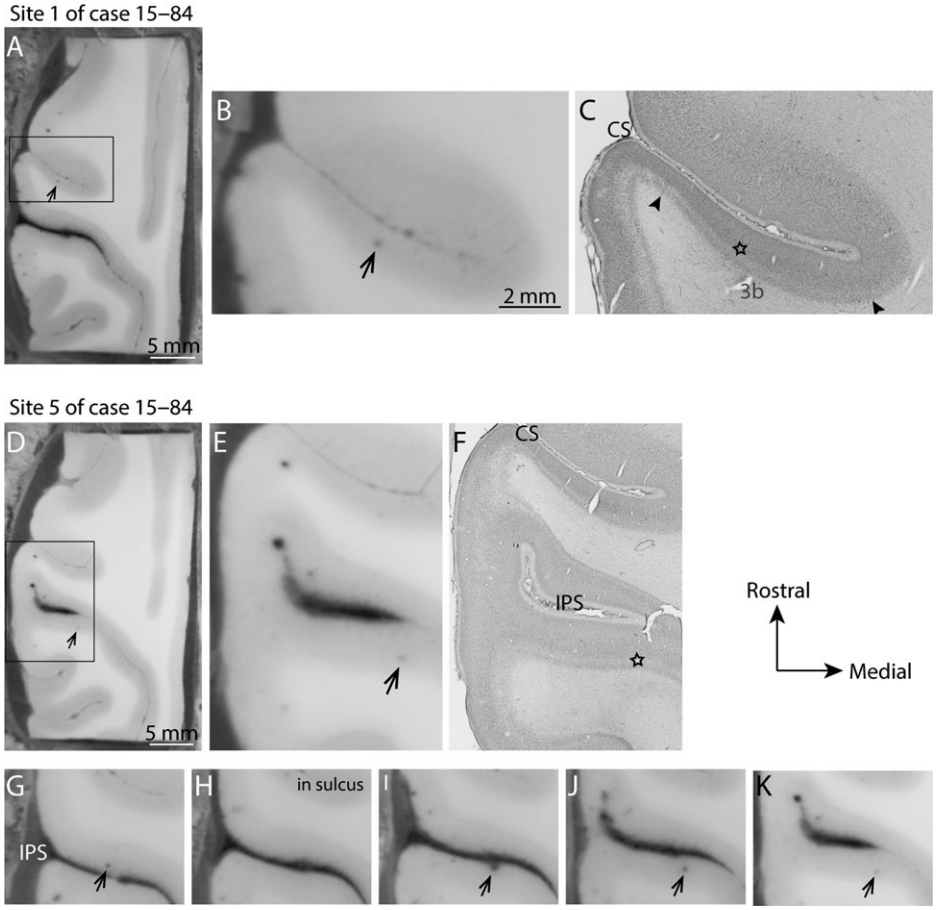

Figure 3. Determination of the location of stimulation sites within the sulcus. Electrode tracks within the sulci were easily identified in our block face images allowing us to determine the depth and location of each penetration site and to directly relate electrode tracks to Nissl-stained sections. This was especially helpful when electrode penetrations progressed deep into the sulcus. These are two examples of electrode tracks in case 15–84. The top row (*A*, *B*, *C*) shows the depth of stimulation site 2 (Fig. 8) within the caudal bank of the central sulcus (CS). (*A*) The block-face image taken during cutting. The darkened dot indicated by the black arrow is the location of a portion of the electrode track. (*B*, *C*) An enlarged portion of the block-face photograph, and a photomicrograph of the same block-face section after it was processed for Nissl substance, respectively. The star indicates the location of the electrode track in the Nissl-stained section, which is in area 3b. The borders of 3b are indicated by the black arrowheads. (*D*–*K*) The progression of the electrode track of site 5 of case 15–84. (*D*, *E*, *F*) The whole block-face, and enlarged views of the block-face and Nissl-stained section respectively. (*G*–*K*) The progression of the electrode track as it crossed the intraparietal sulcus (IPS). Thus, though the penetration site first entered on the medial bank of the IPS in area 5, evoked movements were from the caudolateral bank of the IPS in area 7 (Fig. 8*D*). Movements were only evoked when the electrode was close to or within layer 5.

for constructing maps of sensory (Nelson et al. 1980; Pons et al. 1985; Seelke et al. 2012), auditory and motor cortex (Gould et al. 1986; Qi et al. 2000). While interpolation/tessellation is a commonly used method for generating cortical maps, there are drawbacks. For instance, regions of the brain where few stimulation sites are tested result in large tessellation tile sizes. To overcome this drawback, we have marked every stimulation site so that the reader can appreciate the density of the sites from which maps were constructed. It is important to note that these tessellation tiles do not denote exact borders of movement domains, but merely reflect general regions where a particular movement could be elicited, while the stimulation site locations of the maps indicate the exact location where the particular elicited movement occurred.

Results

We tested 992 sites in motor, anterior parietal cortex, and PPC in 6 macaque monkeys. Movements could be evoked at 678 (68.3%) of these sites (see Table 3 for summary). In addition to movement maps (Figs 4*C* and 6*C*, and Supplementary Fig. S1) across cortical fields we also generated threshold maps (Figs 4*E* and 6*E*, and Supplementary Fig. S2), and maps that focused primarily on digit movements (Fig. 7 and Supplementary Fig. S3). Illustrations of representative movements (Fig. 5) and similar movements across cortical areas are shown in Figs 8 and 9. All stimulation sites were registered to anatomically defined cortical field boundaries (Figs 2 and 10; see Materials and Methods). Neuronal RFs for some sites in areas 1 and 2 were also determined (Fig. 11).

Multiple Movement Representations Within Frontal and Parietal Cortex

One of the most striking results of the current study was the extent of cortex from which movements could be elicited (Figs 4 and 6). Not only were movements evoked from motor fields in frontal cortex (PMC and M1), as expected from previous studies in macaques, but movements were also evoked from a large portion of the PPC (Brodmann's areas 5, 7a, and 7b). While movements have been elicited in PPC in New World monkeys

Downloaded from https://academic.oup.com/cercor/advance-article-abstract/doi/10.1093/cercor/bhx279/4608060
by University of California, Davis user
on 26 March 2018

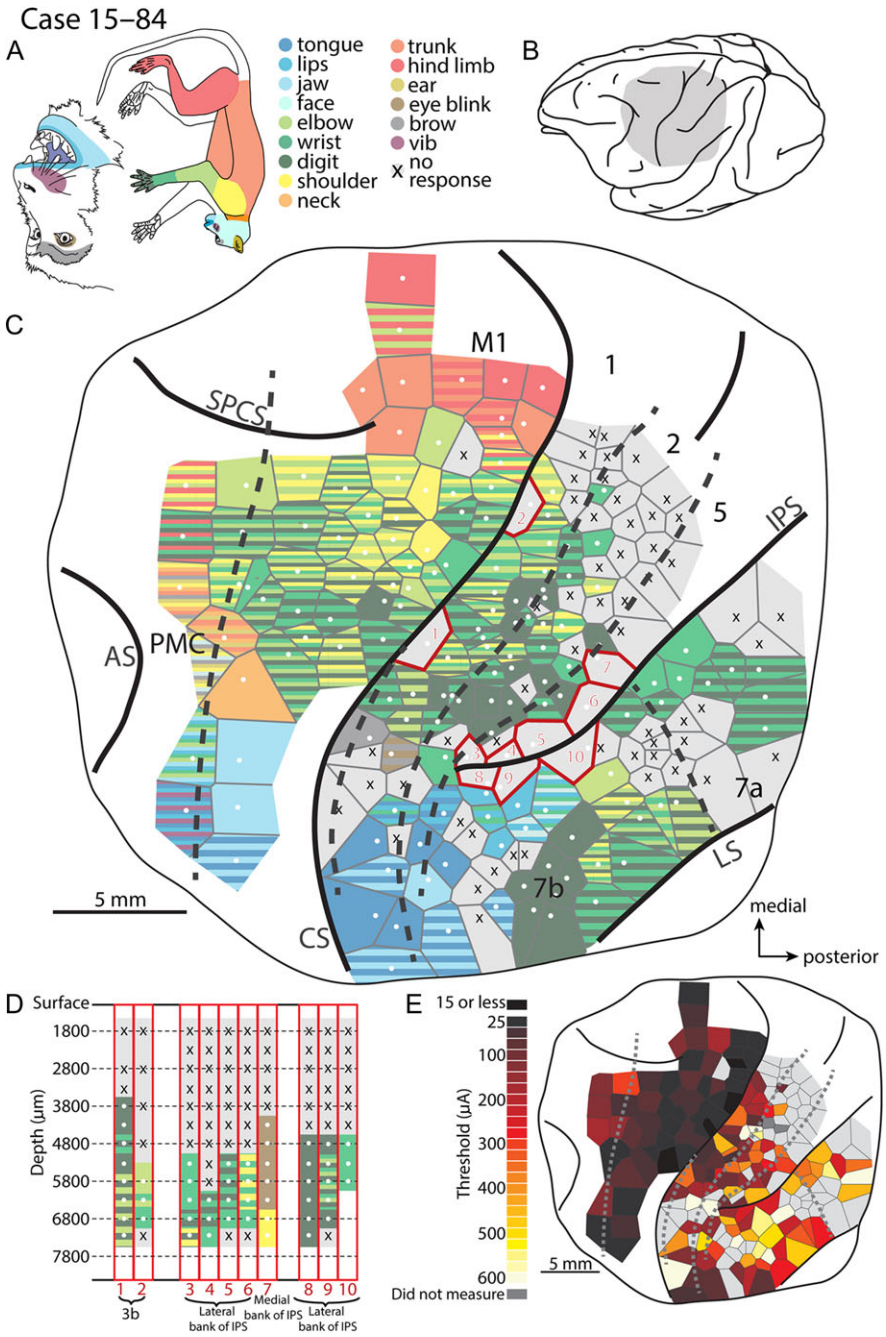

Figure 4. Intracortical microstimulation map for cases 15–84. (*A*) Monkey face and a body with body parts color-coded. (*B*) Lateral view of the macaque brain with the gray shading representing the region mapped using long-train intracortical microstimulation (LT-ICMS) (*C*). (*C*) LT-ICMS map of stimulation sites across motor, parietal and posterior parietal cortex. Dashed lines represent borders of architectonically defined cortical areas while solid lines represent sulci, and the full extent of the craniotomy (thin solid line). White dots represent the electrode penetration sites where movements were elicited. Tiles surrounding the white dots indicate the body part(s) involved in the movement according to the color code in (*A*). Striped Voronoi tiles indicate movements involving multiple body parts. X's in gray Voronoi tiles represent sites where LT-ICMS failed to elicit a movement up to 600 μA. Numbered sites outlined in red were tested at multiple depths within a sulcus. (*D*) Corresponds to these sites and shows the movements elicited at a given depth. Similar to above, white dots and colored tiles represent depths where LT-ICMS evoked movements. X's over gray represent depths where no movement was observed up to 600 μA. Depth is represented along the *Y*-axis while the corresponding site number from (*C*) is indicated along the *X*-axis. Note that movements can be elicited in a far greater expanse of cortex than was previously described (Fig. 1*B*) including areas PMC, M1, 3b, 1, 2 and much of PPC. Further, many of these evoked movements involved the digits, forelimb and shoulder. (*E*) Threshold map for ICMS sites. Where sites were tested at different depths within the sulcus, the lowest threshold is shown. Darker tiles represent low thresholds, while lighter tiles represent high thresholds. Dark gray tiles indicate that a threshold was not measured for a given site, while light gray tiles represent sites where a movement was not observed. The lowest movement thresholds were in PMC and M1 while the highest thresholds were in PPC. Abbreviations are in Table 1.

and prosimian primates (Fig. 1*B*, *D*, *F*) (Kaas et al. 2017), the extent of cortex from which movements could be evoked was more restricted than in the present study. A completely novel finding was that movements could be evoked from somatosensory cortical fields (Figs 4, 6, and Supplementary Fig. S1:3b, 1, and 2), which has not been reported for any primate using LT-

Downloaded from https://academic.oup.com/cercor/advance-article-abstract/doi/10.1093/cercor/bhx279/4608060
by University of California, Davis user
on 26 March 2018

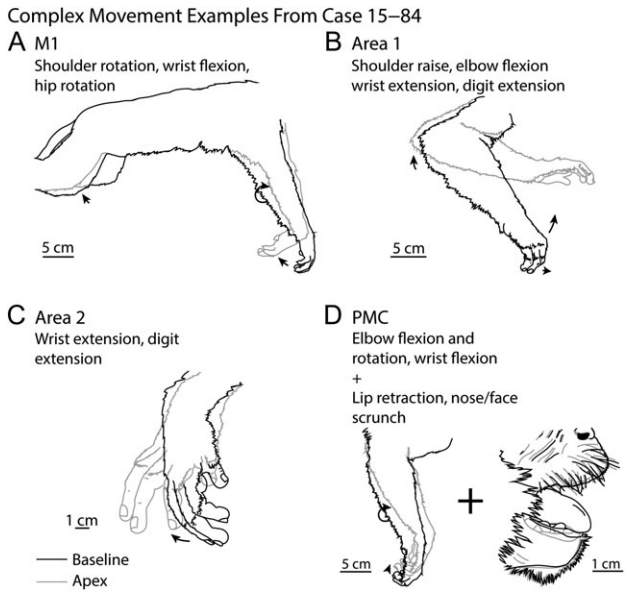

Figure 5. Complex movements. Examples of complex movements evoked from in M1 (*A*), area 1 (*B*), area 2 (*C*), and PMC (*D*) in case 15–84. The baseline posture (prior to stimulation onset) is illustrated in black while the posture at the apex of the movement is illustrated in gray.

ICMS except for a small grasp zone within area 2 in New and Old World monkeys (Fig. 1*H* Gharbawie et al. 2011a, b).

The general organization of movement representations revealed by LT-ICMS was roughly topographic, with movements involving the hind limb represented medially in M1 and PMC, and movements involving the forelimb and face represented in more lateral locations in these fields. We were able to elicit both complex (involving multiple joints and body parts), and simple movements (involving movements around a single joint) from PMC, M1, area 1, and 7b (Fig. 5). However, the complex movements evoked from areas 2, 5, and 7a were limited to movements of a single body part (the forelimb). Though we found complex movements throughout motor and parietal cortex, it was not always easy to assign such movements to the ethological movement categories described by previous investigators (see Graziano 2016 and Kaas et al. 2017 for review), and thus we represent our movement maps based on the body part involved in the movement versus assigning such movements to specific categories (Figs 4 and 6, and Supplementary Fig. S1). Regardless, there are clusters of movements involving similar body parts throughout our maps, and many of these movements are repeated across multiple cortical fields (see, Figs 8 and 9), similar to reports in other primates (see Kaas et al. 2017 for review).

In all cortical fields, we found a large representation of forelimb movements (shoulder, elbow, wrist, and digits), which comprised 535 sites or 78.9% of all sites from which movements could be evoked (Figs 4 and 6, and Supplementary Fig. S1). Many of the forelimb movements were complex in nature such that multiple joints (46.9%) and/or multiple body parts (12.3%) were involved (Figs 4 and 6, and Supplementary Fig. S1). Of all evoked forelimb movements, 60.6% (318) involved the digits.

Digit-Specific Movement Representations

A second major finding of the current study was that movements involving the digits could be evoked from all cortical fields examined. To highlight these movements, and to reveal possible organization patterns, digit-specific movement maps were created. Specifically, maps illustrated whether digit movements were associated with the digits flexing, or extending (Fig. 7 and Supplementary Fig. S3). When focusing on the movements of specific digits we found that many locations within areas 1, 2, 5, 7a and 7b could be segregated into regions in which the evoked movements included all digits (Fig. 7*C*, *E*, and *G*), or only a few digits (Fig. 7*D*, *F*, *H*). Generally, we found that movements involving only 1 or 2 digits were located lateral or rostrolateral to those movements that involved all digits, except in PMC and M1 where movements involving only 1 or 2 digits were evoked less often and were usually somewhat scattered throughout the map (Fig. 7 and Supplementary Fig. S3). However, in 1 case, we found a cluster of single digit extensions (Supplementary Fig. S3B) in a more caudolateral location within M1. Many of the specific digit movements were similar to movements that are common in macaque monkeys such as precision grips and grasps (Macfarlane and Graziano 2009) (Fig. 7*D*, *H*), while those movements involving all digits were reminiscent of full hand grasping or reaching maneuvers (Fig. 7*C*, *E*), including power grasps with D2–5 flexing, and D1 extending (Fig. 7*G*).

Movement Profiles Across Cortical Areas

Although repetitive movements have been reported previously for long duration stimulation techniques in macaques (Vogt and Vogt 1919), tree shrews (Baldwin et al. 2017), and ground squirrels (Cooke et al. 2008), we did not observe such movements in the current study. Instead movements either progressed to their apex (maximum displacement) and maintained that position (Fig. 8*C*), or reached their apex and then returned to baseline prior to the cessation of stimulation (Fig. 9*C*).

Similar evoked movements from different cortical fields were compared to determine if there were noticeable and consistent differences in their movement profiles. Generally, movements in motor cortex reached their apex location more quickly than similar movements in other cortical areas (Fig. 8). We measured movement onset latencies from the video recordings made during the experiment. While we did not observe systematic differences in latency across the cortical fields stimulated, this analysis is limited by the temporal resolution of our video recordings (60 frame/s) and the variability associated with using the start of a noticeable movement (as compared with the latency of EMG activity) as a marker for movement onset.

Movement Thresholds

Threshold values are often used for defining borders between motor areas in frontal cortex, i.e., M1 and PMC (McGuinness et al. 1980; Sessle and Wiesendanger 1982; Weinrich and Wise 1982). Therefore, we measured threshold values for most stimulation sites (see Figs 4*E* and 6*E*, and Supplementary Figs S2 and S4). In the present study; however, we found that determining the border based on threshold values alone, outside of frontal cortex, was not as precise as determining the boundaries of cortical fields using architectonic distinctions (see below). Further, movement threshold values varied with the level of anesthesia. As a result, the variability in threshold values was sometimes quite large within a given cortical area (Figs 4*E* and 6*E*, and Supplementary Figs S2 and S4). Although there were no significant differences in threshold values across

Downloaded from https://academic.oup.com/cercor/advance-article-abstract/doi/10.1093/cercor/bhx279/4608060
by University of California, Davis user
on 26 March 2018

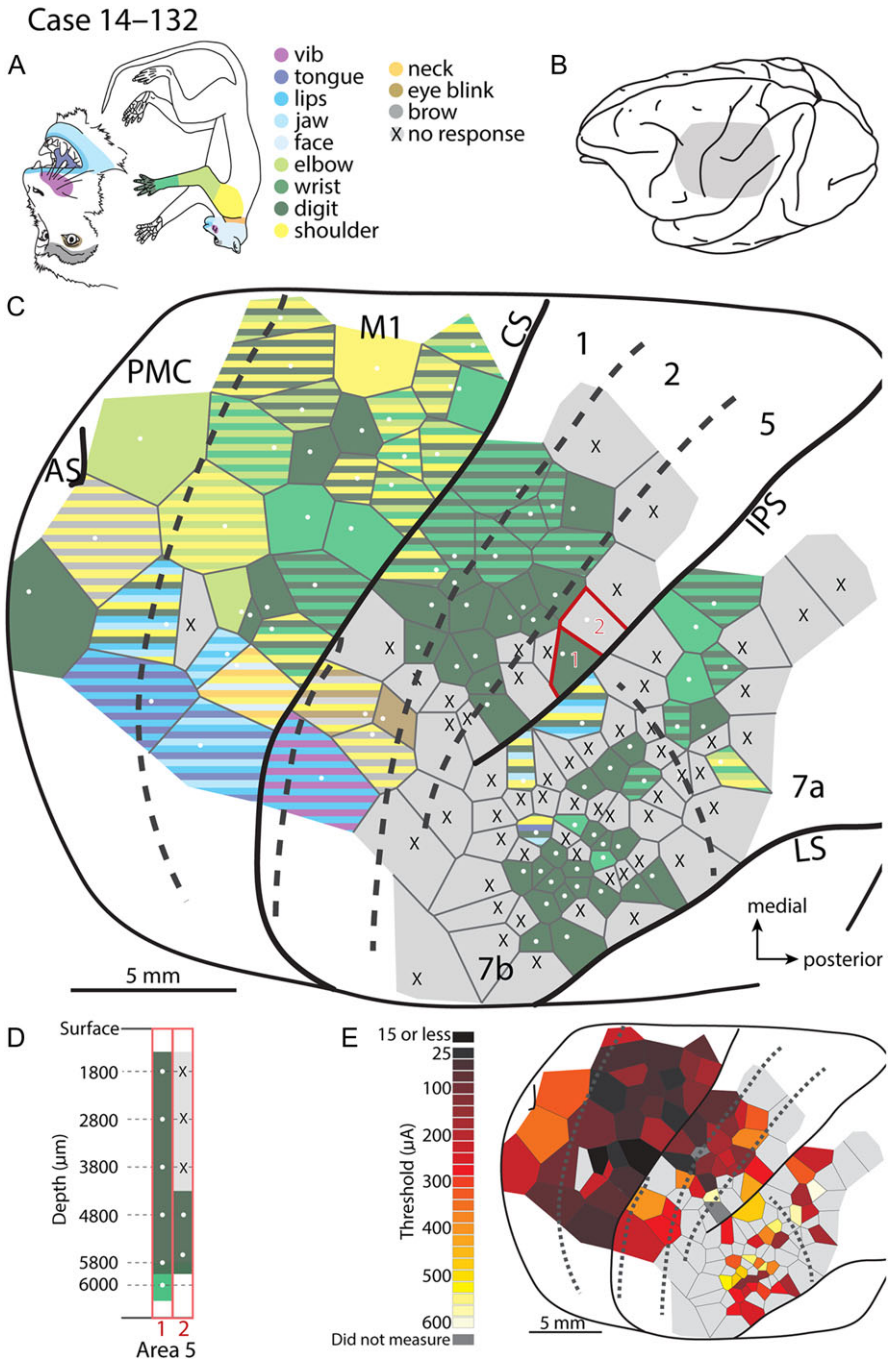

Figure 6. Intracortical microstimulation map for case 14–132. (*A*) Monkey face and a body with body parts color-coded. (*B*) Lateral view of the macaque brain with the gray shading representing the region mapped using long-train intracortical microstimulation (LT-ICMS) (*C*). (*C*) LT-ICMS map of stimulation sites across motor, parietal and posterior parietal cortex. Numbered sites outlined in red were tested at multiple depths within a sulcus. (*D*) corresponds to these sites and shows the movements elicited at a given depth. Depth is represented along the *Y*-axis while the corresponding site number from (*C*) is indicated along the *X*-axis. (*E*) Threshold map for ICMS sites. Where sites were tested at different depths within the sulcus, the lowest threshold is shown. The lowest movement thresholds were in PMC and M1 while the highest thresholds were in PPC. CS is central sulcus, IPS is intraparietal sulcus, AS is arcuate sulcus, LS is lateral sulcus, and SPCS is superior precentral sulcus. Conventions as in Figure 4.

bordering somatosensory areas (i.e. between areas 3b and 1, or areas 1 and 2) and between areas in PPC (areas 7 and 5), we did find significant differences in threshold values between areas bordering the main regions of posterior parietal, anterior parietal, and frontal cortex. For example, we found significant differences in threshold values between primary motor cortex and area 3b ($P = 0.0005$), and between areas 2 and 5 ($P = 0.0106$) (Supplementary Fig. S4). Overall, threshold values were lowest for sites in primary motor cortex (M1: average threshold = 72.5 μA), followed by premotor cortex (PMC: average threshold = 133.4 μA), somatosensory areas (3b, 1 and 2: average combined threshold = 241.0 μA) and PPC (areas 5 and 7: average combined threshold = 337.6 μA), respectively. Thus, the further the site was from M1, the higher the threshold was likely to be.

Downloaded from https://academic.oup.com/cercor/advance-article-abstract/doi/10.1093/cercor/bhx279/4608060
by University of California, Davis user
on 26 March 2018

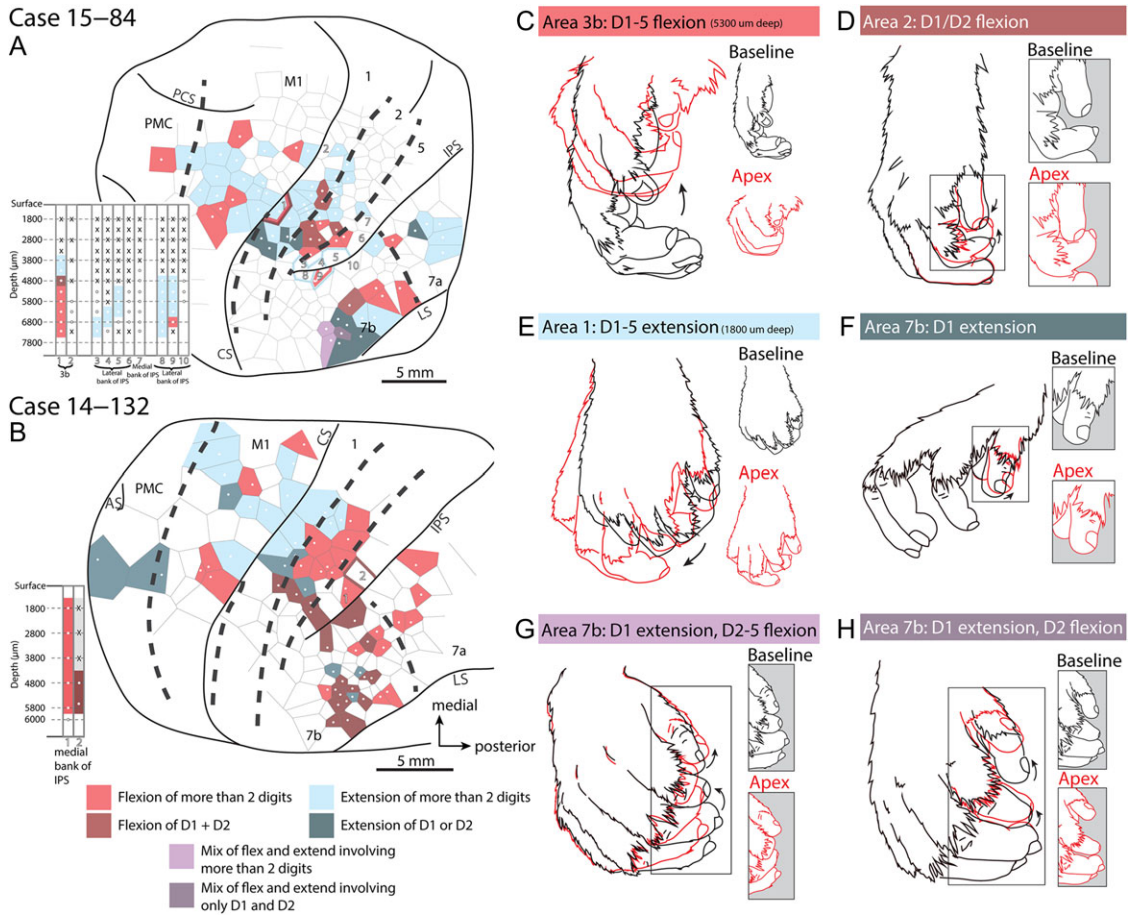

Figure 7. Digit maps. Movement maps for digits for cases 15–84 (*A*) and 14–132 (*B*). The Veronoi tile color corresponds to types of digit movements that were elicited. All other portions of the motor map have been removed such that this map only represents specific digit flexions or extensions. Depth information is provided in the insert to the left of the main maps with each column number corresponding to the penetration site numbers on the map. (*C*–*H*) Examples of different movement types. Black indicates the starting position of the movement, while red represents the apex of the movement. In the maps (*A*, *B*), pink represents sites where ICMS evoked flexion of more than 2 digits such as in a full hand grasp (*C*), while brown tiles represent only D1 (thumb) or D1 and D2 (index finger) flexion, such as in a precision grip (*D*). Light blue represents extension of more than 2 digits (*E*), while dark blue represents sites where only D1 or D1 and D2 extended (*F*). Purple indicates combinations of digit flexions and extensions. Light purple indicates that D1 extension and D2–5 (middle finger to pinky) flexion (*G*). Dark purple indicates extension of D1 with flexion of only D2 (*H*). Conventions as in previous figures.

Movement Maps and Their Relationship to Architectonically Defined Cortical Field Boundaries

We directly related our stimulation data to architectonically defined borders of cortical fields using Nissl-stained sections (Fig. 10) to determine the location of our stimulation sites with respect to cortical field boundaries. The architectonic characteristics of cortical areas have been well described in previous studies (Vogt and Vogt 1919; Jones et al. 1978; Padberg et al. 2009; Seelke et al. 2012) and are only briefly described here. Despite its characteristic architecture with darkly stained pyramidal cells located in layer 5, defining the borders of M1 using architecture alone is difficult. As a result, the rostral border of M1 is often defined based on changes in stimulation threshold values (Sessle and Wiesendanger 1982; Weinrich and Wise 1982; Godschalk et al. 1995). Within the central sulcus and along the medial aspect of the lip of the sulcus, cells are distinctly organized within layer 5; however, at more rostral locations, the cells become somewhat scattered (Fig. 10). Close to the rostral border of area 4, the layer 5 pyramidal cells decrease in size and number and become clustered with large intervening gaps between them. Some have suggested that the rostral border is more clearly indicated by the width and homogeneity of layers 6 and 3 versus using the presence of layer 5 pyramidal cells alone (Vogt and Vogt 1919; Jones et al. 1978), and it is this criterion that was used for the present study.

Area 3b was easily identified on the caudal bank of the central sulcus by densely packed and darkly stained cells in layers 4 and 6. Area 1 had a less conspicuous lamination pattern than area 3b due to less cell packing in layers 4 and 6, and a thicker layer 5. Compared to area 1, area 2 had more densely cell packed layers 3, 5, and 6. Layer 6 also stained more darkly in area 2 compared to area 1. In medial locations, this border was clear, but in lateral locations this border was more difficult to distinguish. Area 5 is marked by more densely packed layers 4 and 5 and a thicker layer 3 that has a lower cell density compared with area 2. The fundus of the IPS was used to demarcate the boundary between areas 5 and 7. The distinction between areas 7a and 7b was based on more densely packed cells in layers 3, 4, and 6 in area 7a compared to area 7b.

While there was some relationship between motor map organization and architectonically defined cortical field boundaries, the co-localization between the two was not precise. For

Downloaded from https://academic.oup.com/cercor/advance-article-abstract/doi/10.1093/cercor/bhx279/4608060
by University of California, Davis user
on 26 March 2018

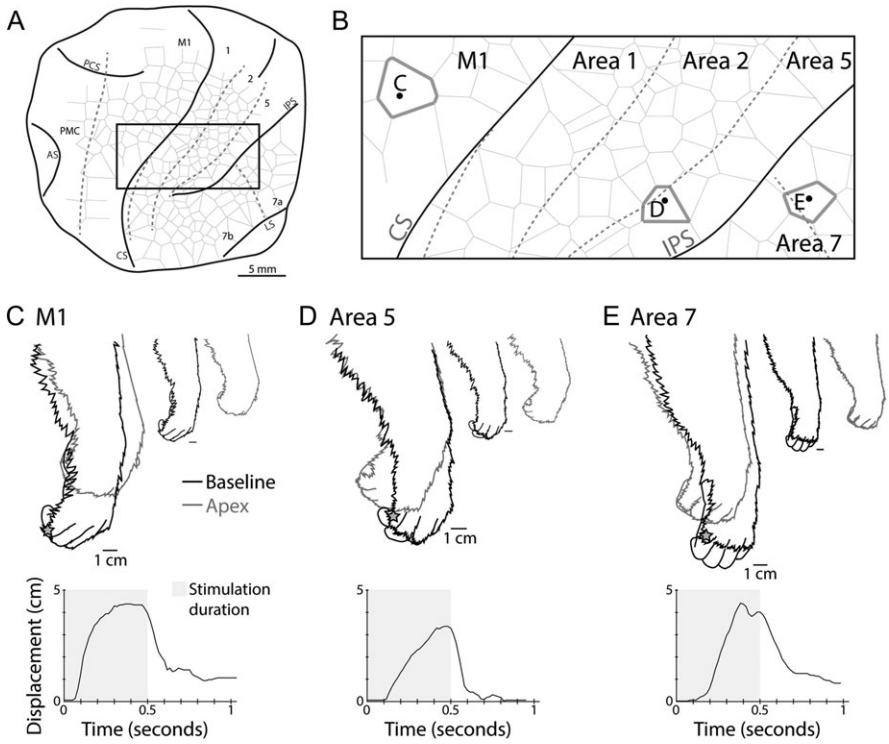

Figure 8. Movement profile comparisons. Comparisons of evoked movements that were similar across primary motor cortex and areas 5 and 7 in case 15–84. (*A*) The outline of the cortex explored and the box indicates the area from which the stimulation sites depicted in (*B*) were taken. Dashed lines indicate borders between cortical areas, while solid black lines indicate the extent of the exposed cortex and the location of sulci, including the central sulcus (CS) and intraparietal sulcus (IPS). (*B*) is a close-up view of the box in (*A*) with the location of example stimulation sites highlighted. The evoked movements shown here involved digit and wrist flexions (*C*–*E*). Black traces in (*C*–*E*) represent the resting position of the hand prior to stimulation (baseline), while gray traces indicate the position of the hand at the maximum displacement (apex) of the evoked movement. Smaller reproductions of these tracings are presented separately at right. The gray star on each tracing indicates the location on the hand used to measure the displacement plotted below each tracing of the hand. The gray shading within the plot represents the period of time LT-ICMS was applied. Movements evoked within M1 tended to reach the apex location earlier in the stimulation epoch and held the position until stimulation stopped.

instance, M1 and PMC had complete representations of the body including the face, trunk, forelimbs, and hind limbs. However, complete representations of movements for the entire body were not observed in all cortical fields. For example, we were unable to elicit movements of the hind limb and trunk from areas 3b, 1, 2, 5, or 7b and were only able to elicit movements of the face and forelimbs. Evoked movements observed in area 7a only involved the forelimb (Figs 4 and 6). It is not clear if anterior parietal areas did not contain movement representations of other body parts or if we did not stimulate medial enough within these representations. Movements of the trunk and or hind limb have been reported in PPC of prosimian and New World Monkeys using LT-ICMS techniques (Gharbawie et al. 2011a; Stepniewska et al. 2005, 2009, 2014).

Correspondence Between Evoked Movements and RFs in Areas 1 and 2

In two cases, RFs determined using electrophysiological recording techniques were directly compared to evoked movements determined utilizing LT-ICMS (Fig. 11). While the somatosensory RF was on the same body part that moved during ICMS, there was not always a precise correspondence between the two. For example, neurons at a site in area 1 had a small RF restricted to distal D3 (Fig. 11B2). The movement evoked from this same site was complex and included an extension of all digits from D1 to D5. At other sites, the location of the somatosensory RF and the elicited movements were more precisely aligned. For instance, the RF of neurons at a stimulation site in area 1 responded to cutaneous stimulation of distal D1, and the evoked movement from this same site was restricted to a D1 flexion (Fig. 11B3).

Discussion

This is the first study in primates using modern microstimulation techniques to demonstrate that complex movements can be evoked from an enormous swath of cortex outside of the boundaries of traditionally defined motor cortex (Fig. 12). In addition to motor and premotor cortex, movements were evoked from areas 3b, 1, 2, 5, and 7. Further, many of the complex movements, involving the forelimb (i.e., reaching- and grasping-like movements) that are represented within motor cortex, are also present within anterior and posterior parietal fields similar to reports in prosimians and New World monkeys (see Kaas et al. 2017 for review). However, one of the major findings of the current study is that when LT-ICMS is used to explore the organization of cortex, macaque monkeys have a far larger region of cortex involved in the production of digit/hand movements compared with species that do not possess an opposable thumb and have less sophisticated hand use.

Other findings of the current study are that threshold values increase the further the stimulation site is from motor cortex. Threshold values for anterior parietal fields are higher than for

Downloaded from https://academic.oup.com/cercor/advance-article-abstract/doi/10.1093/cercor/bhx279/4608060
by University of California, Davis user
on 26 March 2018

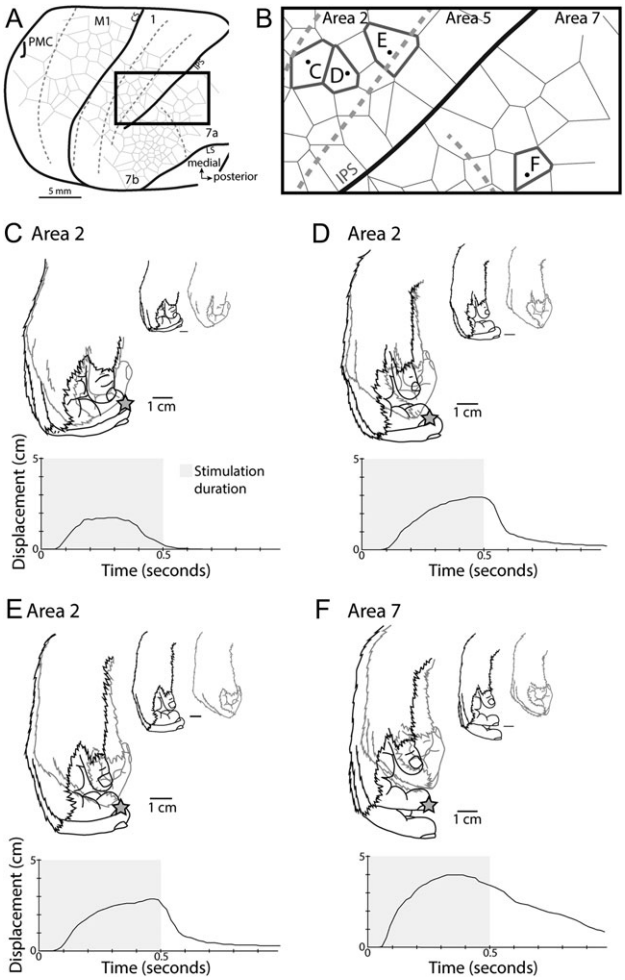

Figure 9. Movement profile comparisons. Comparisons of similar evoked movements in areas 2 and 7a of case 14–132. The time course of movement displacements for sites within area 2 were variable across locations, with one site in rostral area 2 reaching the apex position and then returning to baseline (*C*), while other sites within area 2 held their apex location for the duration of stimulation (*D*, *E*). During stimulation at the area 7a site (*F*), the hand reached the apex location and started to return to baseline prior to stimulation offset. All conventions are as in Figure 8.

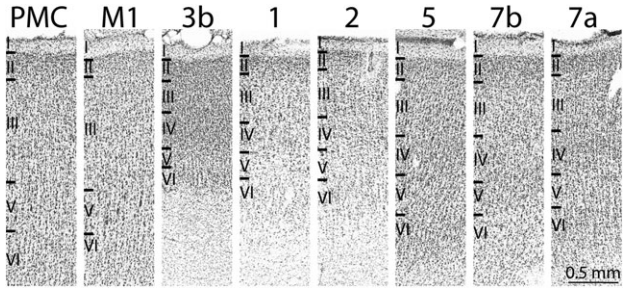

Figure 10. Architectonic borders of cortical fields. Cortical field boundaries were determined by reconstructing a series of horizontal sections stained for Nissl and aligning them with block face images that were then compiled to generate a 3D image of the brain (Fig. 2). The architecture of motor cortex varies across its rostral and caudal extent with caudal portion of M1 containing more precisely aligned layer 5 pyramidal cells. In the rostral portion of M1 these cells become smaller and are more dispersed within layer 5. The exact border between M1 and PMC is difficult to determine architectonically, and varies along the medial/rostral aspect; however, we found that there was a decrease in density and size of layer 5 pyramidal cells, as well as a slight increase in the density of layer 3 and layer 6 cells. This appearance of PMC is consistent with previous reports (Vogt and Vogt 1919; Jones et al. 1978). The boundaries of 3b, 1, and 2 have been well characterized. Located on the caudal bank of the central sulcus, area 3b is identified by densely packed and darkly stained cells in layers 4 and 6. Area 1 can be differentiated from area 3b by less cell packing in layers 4 and 6, and a thicker layer 5. Area 2 has more densely cell packed layers 3, 5, and 6 relative to area 1 and also has a more darkly staining cells in layer 6 compared to area 1. Area 5 is marked by more densely packed layers 4 and 5 and a thicker layer 3 that has a lower cell density compared to area 2 (Seelke et al. 2012). We distinguished areas 5 and 7 using the fundus of the IPS as a border, and did not make further distinctions of the areas that lay within the IPS. Area 7a is distinguishable from 7b by having more densely packed cells in layers 3, 4, and 6.

motor and premotor cortex, and threshold values for PPC are the highest observed. Finally, the topography of motor maps was in rough correspondence with maps in anterior parietal fields, and the location of somatosensory RFs for neurons in layer 4, at the same site as our stimulation, overlapped with the body parts involved in the evoked movements. This suggests that there is a strong correspondence between sensory input and movement output within a given column of cortex.

How Do Our Results Compare With Previous ST-ICMS and LT-ICMS Studies?

A number of studies have used ST-ICMS to evoke movements from both M1 and PMC in a variety of primates including squirrel monkeys, owl monkeys, cebus monkeys, galagos, and macaque monkeys (Kwan et al. 1978; McGuinness et al. 1980; Sessle and Wiesendanger 1982; Weinrich and Wise 1982; Strick and Preston 1982a; Gould et al. 1986; Stepniewska et al. 1993; Godschalk et al. 1995; Wu et al. 2000; Burish et al. 2008; Qi et al. 2010; Milliken et al. 2013; Dea et al. 2016). Our findings on M1 are in good agreement with these previous studies in that we observed a gross topographic organization with the hind limb represented medially followed by representations of the forelimb and face laterally. Like a number of the studies that utilized ST-ICMS, representations were fractured with multiple representations of the same body part movement (e.g., wrist, digits, and shoulder). The number of stimulation sites in PMC was restricted in the present investigation but our findings were consistent with other studies in macaque monkeys (Sessle and Wiesendanger 1982; Godschalk et al. 1995; Dum and Strick 2002) in that representations of the forelimb/digits were just caudal to the arcuate sulcus and the representation of the face was lateral to the arcuate (Fig. 12).

LT-ICMS was originally used to explore motor cortex in macaque monkey by Graziano et al. (2002a, b), and there have been a number of subsequent studies of macaque motor cortex that have used similar techniques (Gharbawie et al. 2011a, b; Griffin et al. 2011, 2014; Overduin et al. 2012). While many of these previous LT-ICMS studies examined a relatively small portion of M1, with most focusing on forelimb movements, the results are consistent with those of the present study. Like these previous studies, we evoked complex movements of the hand and forelimb, including complex grasping movements on the precentral gyrus between the arcuate and the central sulcus (Fig. 12*C*). In the studies of Graziano et al. (2005) and Gharwabie et al. (2011b) in which M1 and PMC were more extensively explored, the gross topographic organization of M1 was much like that of the present study. Similar to these previous studies, movements evoked from PMC in the present investigation were often complex and included multiple joints and body parts.

Downloaded from https://academic.oup.com/cercor/advance-article-abstract/doi/10.1093/cercor/bhx279/4608060
by University of California, Davis user
on 26 March 2018

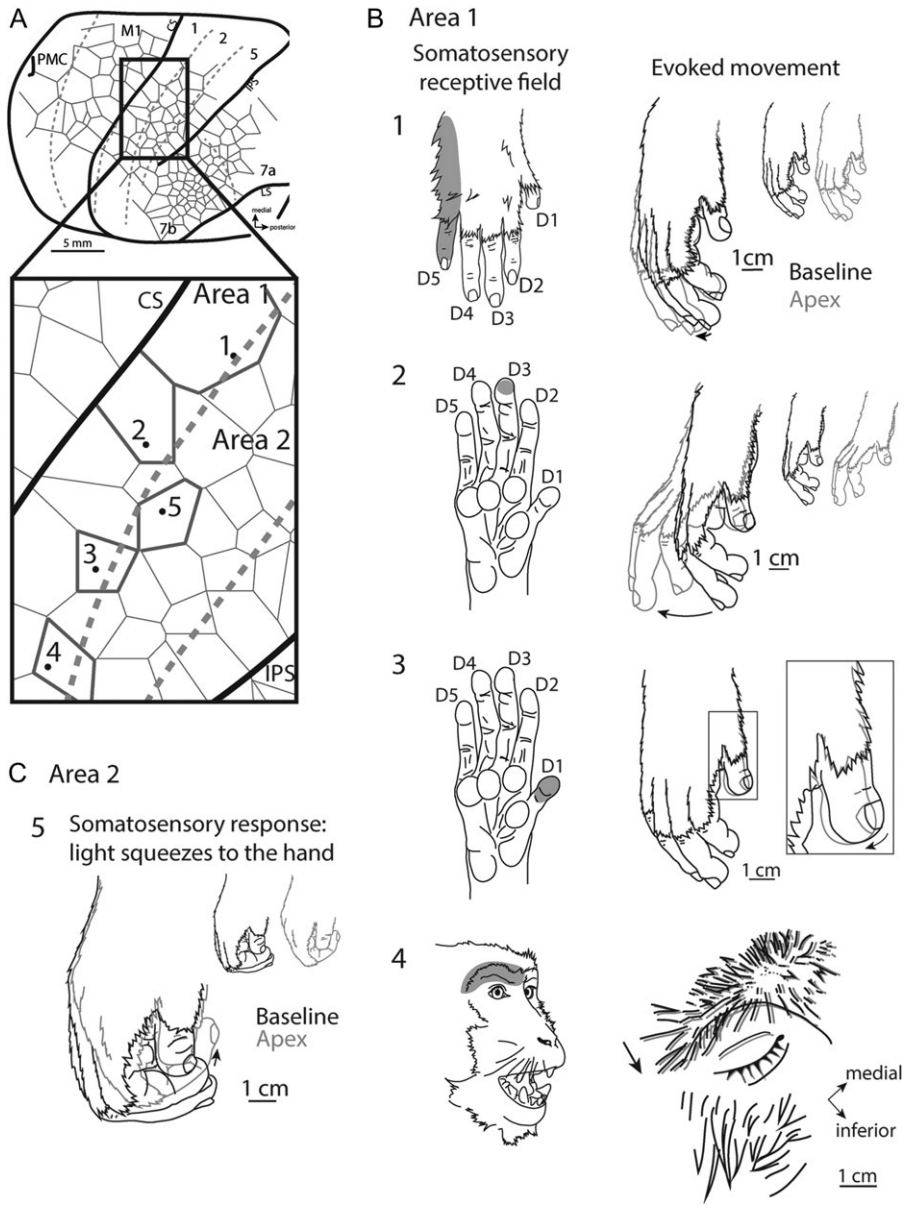

Figure 11. Overlap of receptive fields and movement fields in areas 1 and 2. A comparison of sensory receptive fields determined with electrophysiological recording techniques with LT-ICMS-evoked movements (movement fields) in the same penetration sites in case 14–132 (Fig. 6). (*A*) depicts the total area explored, with an enlarged inset showing example sites. (*B*) Comparisons of receptive fields (left) on the hand (1–3) and face (4) for sites in area 1 with evoked movements from the same locations (right). At some sites movements evoked included portions of the hand that were not part of the receptive field (e.g., B2), while at other sites the receptive field location and the body parts involved in the evoked movements had a closer correspondence (e.g., B3 and 4). For area 2, light squeezes to the hand evoked a response while LT-ICMS evoked D1–5 digit flexion ("grasp").

As noted in the introduction, previous studies utilizing LT-ICMS in macaque monkeys have reported evoked movements from limited portions of PPC such as LIP (eye movements (Thier and Andersen 1998)), and VIP (defensive movements (Cooke et al. 2003), a small region in area 2 (grasping movements (Gharbawie et al. 2011b)), and a small region within area 5 (digit movements (Rathelot et al. 2017)). Studies in which LT-ICMS was used to examine PPC in prosimians and New World monkeys found that movements could be evoked from the rostral portion of PPC (termed PPCr; possibly corresponding to portions of area 5 in macaque monkeys), but these studies did not demonstrate that movements could be evoked from anterior parietal areas such as areas 3b, 1 and 2. Studies in New World monkeys and galagos grouped similar movements into ethologically relevant movement "domains" such as grasping, hand-to-mouth, and defensive movements (Graziano 2016; Kaas et al. 2017).

Our study differs from these previous studies not only in the amount of cortex from which movements could be evoked, but also in the diversity of cortical locations from which movements of the forelimb and specifically the digits could be evoked. In fact, one of the most significant findings of the present investigation is the discovery of clustered representations of only D1 and/or D2 movements in PPC, somatosensory cortex and frontal motor areas (Fig. 7 and Supplementary Fig. S3). Equally important are the multiple representations of a variety

Downloaded from https://academic.oup.com/cercor/advance-article-abstract/doi/10.1093/cercor/bhx279/4608060
by University of California, Davis user
on 26 March 2018

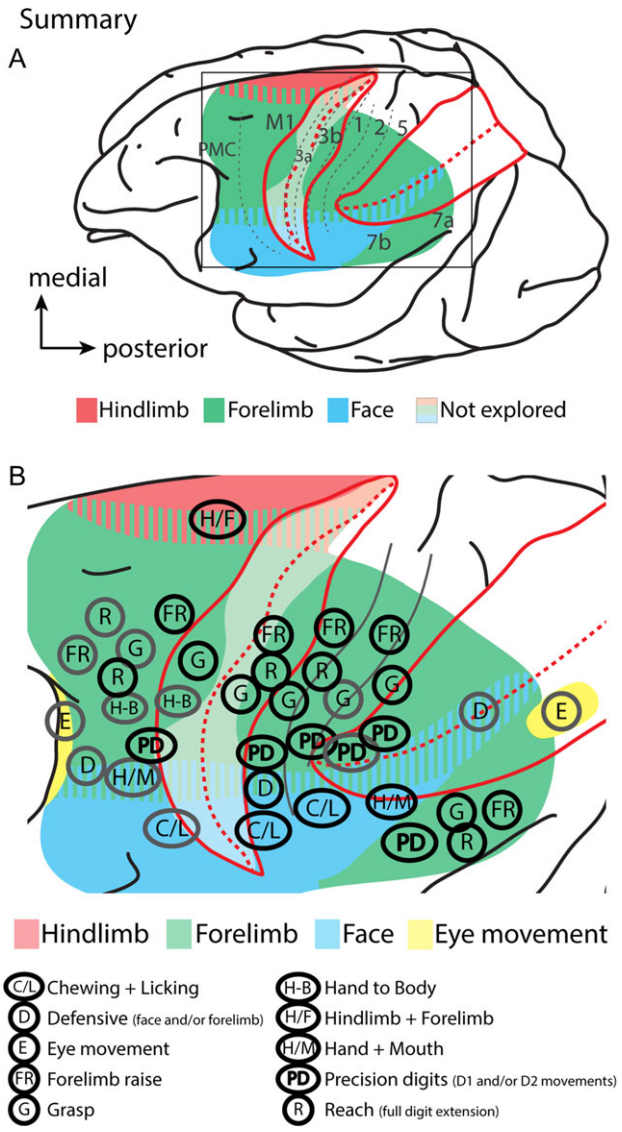

Figure 12. Summary of findings. (*A*) The extent and gross topography of cortex from which movements could be evoked using LT-ICMS in macaque monkeys. The IPS and the central sulcus are opened. Different colors indicate the general topography of the movement maps. The translucent white region in the CS indicates regions that have not been explored using LT-ICMS. (*B*) is an expanded view of the boxed region in (*A*) showing the location of movement domains in reference to "ethological movement" classifications (*B*). Though, we wish to choose an agnostic classification of movement domains/clusters, we tentatively assign the observed clusters in the present study to previously described ethological movement categories for comparative purposes. Ethological designations are based on observing multiple adjacent sites with similar movements and our designations do not reflect all possible ethological movements that were observed (i.e., if a particular movement was only observed at a single stimulation site across all cases) or that may be present. Gray circles indicate those movements that have been previously described (Fig. 1), while black circles indicate movement representations revealed in the current study. Unlike other primates examined, motor, anterior and posterior parietal fields have distinct representations of D1 and D2 movements (indicated as "PD" in (*B*)). Though more precise digit movements involving D1 and/or D2 are likely present within the central sulcus (in M1 and areas 3a and 3b) we did not explore this region well enough to indicate the location or extent of such movements. Summary figures are based on data from the present study, as well as data from Graziano et al. (2002a, b), Cooke et al. (2003), Thier and Andersen (1998), Gharbawie et al. (2011a, 2011b), and Rathelot et al. (2017).

of complex digit movements that correspond to a number of grip types and hand manipulations that surround the D1/D2 clusters. While the majority of movements evoked from PPC were complex in that they involved multiple joints (i.e. wrist and elbow), digits (D1 + D2, or D1–D5), or body parts (jaw + digits + wrist), we did not assign the observed movements to ethologically relevant movement categories (Fig. 12*B*). Rather, we took an agnostic view and clustered sites that contain similar body part kinematics (Figs 4 and 6, and Supplementary Fig. S1). Another difference between LT-ICMS maps in prosimian and New World Monkeys from our own results is that we were unable to elicit movements from the trunk or hind limb within PPC. Whether this is because we did not test enough medial sites where such movements might be present, because of differences in anesthesia or average threshold values required to stimulate within PPC, or because such representations are not present in macaques is uncertain. Regardless, the results of the current study support electrophysiological studies that demonstrate that PPC is involved in the cortical control of complex forelimb and hand movements in macaque monkeys (see below), and also indicate that anterior parietal fields not only provide proprioceptive and tactile feedback necessary for motor control, but also may play a more direct role in the generation and modulation of movements.

Somatosensory Cortex May be Involved in Motor Control

Unlike PPC, the notion that somatosensory cortex, including areas 3a, 3b (S1), 1 and 2, is involved in generating and modulating movement is not universally accepted. As noted in our introduction, early studies of the 1800 and 1900s demonstrated that movements could be evoked from somatosensory cortex in primates (including humans). In modern studies using ICMS techniques, movements could be evoked from areas 3a and portions of 3b in galagos (Wu et al. 2000), marmosets (Burish et al. 2008), tree shrews (Baldwin et al. 2017), and squirrels (Cooke et al. 2015).

Lesion studies also suggest that in addition to their role in tactile discrimination and proprioception, anterior parietal areas also play a role in movement execution. For example, lesions to motor areas do not permanently abolish movement (Rouiller et al. 1998), and early surface electrode studies demonstrate that movements can be evoked from somatosensory cortex after motor cortex is ablated (Kennard and Mc Culloch 1943; Woolsey et al. 1953; Fleming and Crosby 1955). Further, in macaques, lesions involving frontal motor areas and anterior parietal areas result in more severe hand movement deficits directly after the lesion, and animals have a slower/poorer recovery of function as opposed to animals with lesions restricted to M1 and PMC (Darling et al. 2016). Similar findings have also been reported in humans. Interestingly, in cases with damage extending into area 2, deficits specifically associated with fine hand manipulations persist (Abela et al. 2012). Finally, a recent electrocorticography study indicates that anterior parietal cortex and PPC are active during voluntary movements in stroke patients with lesions to motor cortex (Godlove et al. 2016).

It is uncertain what pathway, or pathways are involved in the production of elicited movements from somatosensory areas; though there are multiple corticocortical, corticobrainstem, corticothalamic, corticothalamocortical as well as direct

Downloaded from https://academic.oup.com/cercor/advance-article-abstract/doi/10.1093/cercor/bhx279/4608060
by University of California, Davis user
on 26 March 2018

corticospinal pathways through which anterior parietal cortical areas could control and modulate movements. For example, in macaque monkeys, areas 2 and 3a have direct connections with primary motor cortex (Pons and Kaas 1986; Gharbawie et al. 2011b), and though connections between M1 and 3b are absent or weak (Jones et al. 1978; Gharbawie et al. 2011b), area 3b along with areas 3a, 1, and 2 have projections to the spinal cord (Toyoshima and Sakai 1982; Nudo and Masterton 1990; Galea and Darian-Smith 1994; Rozzi et al. 2006). In fact, approximately 23% of the corticospinal tract neurons are located posterior to primary motor cortex (Toyoshima and Sakai 1982). The existence of direct projections of cortical cells onto motoneurons in the spinal cord has not been reported outside of a portion of M1 and area 3a in macaque monkeys (Rathelot et al. 2006, 2009). (Widener and Cheney 1997). Yet, single-pulse and repetitive pulse ICMS stimulation of areas 3b, 1, and 2 do affect recorded muscle activity (Widener and Cheney 1997), suggesting that these cortical fields likely influence the generation and execution of movements through multisynaptic pathways. Recent evidence from Rathelot et al. (2017) has shown that area 5 may influence movement production indirectly through interneurons in the spinal cord. Other potential pathways for anterior and posterior parietal cortical areas to influence motor output include connections through the striatum (Jones et al. 1977), or the corticopontocerebellar system (Vassbo et al. 1999).

The Correspondence Between Motor Maps and Somatosensory Maps

An obvious question is whether movement maps generated with LT-ICMS are in register with the topography of somatosensory maps in anterior parietal areas. A related question is whether these motor representations can be directly related to the architectonic boundaries of cortical areas, as are somatotopic maps in areas 3a, 3b, 1, and 2. A distinct feature of somatosensory maps in areas 3b and 1 of macaque monkeys is that they are exceptionally precise, contain neurons with small RFs (particularly on the hand), have relatively little variability in organization across individuals, and have a clear relationship to cortical architecture (Nelson et al. 1980; Pons et al. 1985; Krubitzer et al. 2004).

Although the density of stimulation sites was different in the different anterior parietal fields across cases in the present study, there were several features of our motor maps that could be distilled. First, we demonstrated that RFs determined using electrophysiological recording techniques were often on the same portion of the body from which movements were evoked, but there was not always an exact correspondence between RFs and evoked movements (Fig. 11). Second, there was a gross topographic organization of our movement maps that roughly aligned with somatosensory maps such that movements of the forelimb/hand were represented medial to movements of the mouth, lips, and face (Nelson et al. 1980; Pons et al. 1985: Krubitzer et al. 2004). Third, the movement maps that spanned somatosensory cortex did not appear to be directly related to the architectonic boundaries that define the functional maps of areas 3a, 3b, 1, and 2, but the presence of such a correspondence may require higher density maps. Fourth, the details of the movement maps in anterior parietal cortex, as well as in motor cortex and PPC, were highly variable across animals, much more so than topographic maps of somatosensory areas (3a, 3b, 1, and 2). Thus, directly comparing maps with different degrees of variation is problematic.

This variability may be due to the dynamic use of the skin versus muscles when these sensory and motor maps are developing. Since the skin covering the muscles, bones, and joints is topographically invariant, one might expect little variability in topographic maps of the skin across individuals; and this appears to be the case for areas 3b and 1. In contrast the degrees of freedom of possible movements of the limbs and digits during development is high, and this may contribute to the higher variability in movement map organization observed across individuals (Figs 4 and 6, and Supplementary Fig. S1).

Relationship Between ICMS, Electrophysiological Recording, and Anatomical Connections in PPC

There is a plethora of electrophysiological data in macaque monkeys, beginning with the seminal work of Vernon Mountcastle (Mountcastle et al. 1975), implicating multiple cortical fields, located in Brodmann's area 5, in coding reach intention (Snyder et al. 1997; Debowy et al. 2001; Calton et al. 2002), reach and grasp kinematics (Kalaska 1996; Wise et al. 1997), monitoring and shaping different reach postures during object approach (Gallese et al. 1994; Sakata et al. 1995; Gardner et al. 2007a, 2007b; Chen et al. 2009), and the coordinate transformation of reach targets into body- and shoulder-centered coordinates (Ferraina and Bianchi 1994; Lacquaniti et al. 1995; Seelke et al. 2012). One study, in which functional sensory maps of the body were generated in area 5 demonstrates that unlike anterior parietal fields, maps are fractured (Seelke et al. 2012). Our ICMS data from PPC are in good correspondence with electrophysiological recording studies in two significant ways. First, our motor maps are dominated by movement representations of the forelimb, hand, and digits. Second, our maps are fractured with the movements represented in multiple clusters, surrounded by clustered representations of related movements (Seelke et al. 2012).

The types of evoked movements we observed from areas 7a and 7b were similar in nature to data from electrophysiological studies of area 7. Specifically, neurons in area 7a are responsive to eye movements and arm movements related to reaching and grasping (Rozzi et al. 2008), while neurons in area 7b are responsive to somatosensory stimulation of the arm, hand, and mouth, and during movements of the hand and orofacial structures (Yokochi et al. 2003; Rozzi et al. 2008; Bonini et al. 2011). In the current study, in rostral portions of area 7b we evoked movements of the jaw and tongue (like chewing and licking). Posterior to this we evoked hand and mouth movements. Near the border between 7a and 7b we evoked full hand grasps and reaching movements.

Our observations of ICMS movements evoked from the different areas that comprise PPC are in good correspondence with anatomical data and deactivation studies in monkeys. For example, in all primates examined, areas 5 and 7b have strong connections with motor areas in frontal cortex (Matelli and Luppino 2001; Padberg et al. 2005; Burman et al. 2008; Stepniewska et al. 2009a; Gharbawie et al. 2011a, 2011b; Bakola et al. 2013). Further, both areas 5 and at least portions of area 7b have direct connections with the spinal cord (Coulter and Jones 1977; Nudo and Masterton 1990; Galea and Darian-Smith 1994; Rathelot et al. 2017), and connections with subcortical structures associated with motor processing (Keizer and Kuypers 1989; Rozzi et al. 2006; Gharbawie et al. 2010). The high threshold values for evoking movements from PPC suggest that the pathway through which the motor signals propagate are likely multisynaptic and less powerful than those from M1.

Downloaded from https://academic.oup.com/cercor/advance-article-abstract/doi/10.1093/cercor/bhx279/4608060
by University of California, Davis user
on 26 March 2018

Recent studies in owl monkeys, squirrel monkeys and galagos indicate that the connections with motor cortex strongly influence rostral PPC (possibly homologous to area 5) in that deactivation of motor cortex in most instances abolish evoked movements in rPPC (Stepniewska et al. 2014; Cooke et al. 2015).

Long- Versus Short-Train Intracortical Microstimulation

One of the main goals of the present study in macaque monkeys was to obtain comprehensive movement maps from different cortical areas and compare our results with those previously reported in other primates (see Kaas et al. 2017 for review), and their close relatives (tree shrews; see Baldwin et al. 2017), to gain insights into the evolution of frontoparietal networks involved in reaching and grasping. Our decision to use LT-ICMS was based on two important considerations. The first was the fact that it is difficult to evoke movements from anterior parietal cortex and PPC using standard short duration stimulation methods. The second reason is that LT-ICMS can evoke movements in anterior parietal cortex and PPC in anesthetized preparations. Therefore, LT-ICMS can be used to compare motor and parietal cortex organization in a variety of species where matching and comparing awake behaving paradigms across species is difficult.

Although it has been argued that a physiological realistic model of motor activation requires LT-ICMS (Graziano et al. 2002b), the interpretations of the organization and function of motor networks determined using LT-ICMS is not without controversy. One critique of LT-ICMS is that the high current amplitudes artificially elicit complex movements due to current spread (Strick 2002). However, there are several studies that indicate that regardless of the duration or amplitude, cortical stimulation activates interconnected networks. For example, one study that combined optical imaging with stimulation demonstrated that LT-ICMS in PPC activates somatotopically matched portions of M1 that are known to be anatomically connected with PPC (Stepniewska et al. 2011). Another study combining biphasic stimulation and optical imaging of the stimulation site in S1, found that increasing the duration and amplitude of current did not result in a simple concentric spread of current around the stimulation site. Rather, activation increased within a patchy pattern surrounding the stimulation site (see Fig. 4 of Brock et al. 2013), to locations that were likely anatomically connected to the stimulation site (Brock et al. 2013).

Anatomical studies of primary motor cortex in monkeys and cats demonstrate that connections link related, but not identical, movement representations. In macaque monkeys, Huntley and Jones (1991) observed a lattice like pattern of intrinsic connections that link representations of different movements (as defined using ST-ICMS) such as the digits and wrist, the digits and shoulder, and the digits and elbow. Similar findings have also been reported in cats (Capaday et al. 2009). Because of these findings, it has been proposed that these heterotopic-muscle/joint networks couple and control muscles involved in multijoint movements, rather than each muscle or joint being controlled individually (Capaday et al. 2013).

It is still uncertain if any pattern of electrical stimulation of the brain captures or sufficiently mimics the biological mechanisms that normally play out within the central nervous system in a behaving animal, even though the resulting movements themselves mimic naturalistic behaviors (Graziano et al. 2002a, b; Gharbawie et al. 2011a, 2011b; Overduin et al. 2012, 2014). Indeed, another criticism, based on EMG recordings resulting from LT-ICMS cortical stimulation is that the long duration stimulation method "highjacks" natural muscle activity and does not reflect naturally occurring movements (Griffin et al. 2011; 2014). Other studies using similar methods have provided alternative conclusions (Graziano et al. 2004; Overduin et al. 2012, 2014 but see Amundsen Huffmaster et al. 2017). While the issues regarding how LT-ICMS affects ongoing EMG activity are pertinent and interesting for understanding motor networks, and specifically, the role cortex plays in generating movement, the questions these types of studies address are different than those of the current study.

Given the overall goals of the current investigation, LT-ICMS is an appropriate technique for exploring and comparing movement representations across species, and this becomes clear when comparing LT-ICMS maps with movement maps generated using different temporal parameters of stimulation. In a recent study in tree shrews (Baldwin et al. 2017), we found that short-train stimulation (50 ms) produced truncated versions of the movements produced with long-train stimulation (500 ms); as noted in the earlier study in macaque monkeys where modern LT-ICMS techniques were utilized (Graziano et al. 2002a, b). Further, the evoked movements did not change for ultra-long train stimulation (800 ms) compared with LT-ICMS (500 ms). Instead, movements simply went through additional repetitions or maintained their apex position for the extended time of stimulation.

Interpreting LT-ICMS Data

Several laboratories have proposed that a fundamental organizational feature of motor cortex and PPC is the representation of ethologically relevant behaviors that an animal deploys (see Graziano 2016 for review). However, the notion of an ethologically relevant movement as a compositional element for movement construction seems somewhat limiting, since what could be considered ethologically relevant can change so rapidly, even within the lifetime of an individual. For instance, the human brain did not evolve to text, use keyboards, or play musical instruments, nor did macaque monkeys evolve to use joysticks, press levers, or touch computer screens; yet they can. Categories of movements appear to be present, but movements within these categories are much more multifaceted than the categorical ethological names may account for. For instance, "grasping" movements involve more than simple full digit flexions, and include other grasp-like movements such as power grasps with the extension of D1 and the flexion of D2–5, precision grips involving D1 and D2, and other digit manipulations such as D1 extension, and D2 flexion (Figs 4 and 6). In the course of learning new motor routines, these clustered representations, or effector synergies, could be combined to generate an enormous range of different manual behaviors, including those unique to recent human history such as typing on a keyboard or playing a piano. In fact, it has been proposed by several laboratories that like the spinal cord, the neocortex has fundamental building blocks or "primitives" that represent spatiotemporal muscle synergies (Flash and Hochner 2005; Overduin et al. 2015) and that these representations can be dynamically, and combinatorially linked through recurrent intrinsic connections to generate a variety of novel (and ethologically relevant) movements (Capaday et al. 2013).

Of all the movements evoked, probably the most interesting were those associated with precision and power grips. While these types of movements have been previously evoked from primary motor cortex and area 5 using ICMS techniques (Gaziano et al. 2005; Gharbawie et al. 2011b; Overduin et al. 2012; Rathelot et al. 2017), this is the first time multiple

Downloaded from https://academic.oup.com/cercor/advance-article-abstract/doi/10.1093/cercor/bhx279/4608060
by University of California, Davis user
on 26 March 2018

representations of different grip types have been reported in somatosensory cortex and multiple locations in PPC in macaque monkeys utilizing ICMS. It is not surprising that some of these movement profiles have not been described in other primates like owl monkeys and galagos because these primates do not have hands with opposable thumbs, and thus do not utilize precision grips in which the thumb is independently opposed to D2 or other digits. In this sense, evoked movements involving only D1 and/or D2 in macaque monkeys could be considered species-specific. Thus, when considering the variety of digit movements that could be evoked (Fig. 7), an ethologically relevant term like "grasping" fails to do justice to the exquisite precision and diversity of the movement types that actually exist.

Supplementary Material

Supplementary data is available at *Cerebral Cortex* online.

Funding

National Institutes of Health, National Institute for Neurological Disorders and Stroke (grant number R01 NS035103) to L.K., NIH NEI (grant number T23 EY015387) to M.K.L.B. and A.B.G., and National Institute for Neurological Disorders and Stroke (grant number F32 NS093721-01) to M.L.K.B.

Notes

We thank Dr Rhonda Oates-O'Brien, Adam Gordon, Jeffrey Padberg, Deepa Ramamurthy, James Dooley, and Carlos Pineda for experimental assistance, and Michaela Donaldson for histological and experimental assistance. *Conflict of Interest*: None declared.

References

Abela E, Missimer J, Wiest R, Federspiel A, Hess C, Sturzenegger M, Weder B. 2012. Lesions to primary sensory and posterior parietal cortices impair recovery from hand paresis after stroke. PLoS One. 7:e31275.

Amundsen Huffmaster SL, Van Acker GM 3rd, Luchies CW, Cheney PD. 2017. Muscle synergies obtained from comprehensive mapping of the primary motor cortex forelimb representation using high-frequency, long-duration ICMS. J Neurophysiol. 118(1):455–470.

Asanuma H, Rosen I. 1972. Functional role of afferent inputs to the monkey motor cortex. Brain Res. 40:3–5.

Bakola S, Passarelli L, Gamberini M, Fattori P, Galletti C. 2013. Cortical connectivity suggests a role in limb coordination for macaque area PE of the superior parietal cortex. J Neurosci. 33:6648–6658.

Baldwin MK, Cooke DF, Krubitzer L. 2017. Intracortical microstimulation maps of motor, somatosensory, and posterior parietal cortex in tree shrews (*Tupaia belangeri*) reveal complex movement representations. Cereb Cortex. 27: 1439–1456.

Bao S, Chen VT, Merzenich MM. 2001. Cortical remodeling induced by activity of ventral tegmental dopamine neurons. Nature. 412:79–83.

Bonazzi L, Viaro R, Lodi E, Canto R, Bonifazzi C, Franchi G. 2013. Complex movement topography and extrinsic space representation in the rat forelimb motor cortex as defined by long-duration intracortical microstimulation. J Neurosci. 33: 2097–2107.

Bonini L, Serventi FU, Simone L, Rozzi S, Ferrari PF, Fogassi L. 2011. Grasping neurons of monkey parietal and premotor cortices encode action goals at distinct levels of abstraction during complex action sequences. J Neurosci. 31:5876–5886.

Brock AA, Friedman RM, Fan RH, Roe AW. 2013. Optical imaging of cortical networks via intracortical microstimulation. J Neurophysiol. 110:2670–2678.

Brown AR, Teskey GC. 2014. Motor cortex is functionally organized as a set of spatially distinct representations for complex movements. J Neurosci. 34:13574–13585.

Burish MJ, Stepniewska I, Kaas JH. 2008. Microstimulation and architectonics of frontoparietal cortex in common marmosets (*Callithrix jacchus*). J Comp Neurol. 507:1151–1168.

Burman KJ, Palmer SM, Gamberini M, Spitzer MW, Rosa MG. 2008. Anatomical and physiological definition of the motor cortex of the marmoset monkey. J Comp Neurol. 506:860–876.

Calton JL, Dickinson AR, Snyder LH. 2002. Non-spatial, motor-specific activation in posterior parietal cortex. Nat Neurosci. 5:580–588.

Capaday C, Ethier C, Brizzi L, Sik A, van Vreeswijk C, Gingras D. 2009. On the nature of the intrinsic connectivity of the cat motor cortex: evidence for a recurrent neural network topology. J Neurophysiol. 102:2131–2141.

Capaday C, Ethier C, Van Vreeswijk C, Darling WG. 2013. On the functional organization and operational principles of the motor cortex. Front Neural Circuits. 7:66.

Chen J, Reitzen SD, Kohlenstein JB, Gardner EP. 2009. Neural representation of hand kinematics during prehension in posterior parietal cortex of the macaque monkey. J Neurophysiol. 102:3310–3328.

Cooke DF, Padberg J, Zahner T, Grunewald B, Krubitzer L. 2008. Complex movements evoked by microstimulation of motor cortex in the California ground squirrel (*Spermophilus beecheyi*). Soc Neurosci. 277.18.

Cooke DF, Padberg J, Zahner T, Krubitzer L. 2012. The functional organization and cortical connections of motor cortex in squirrels. Cereb Cortex. 22(9):1959–78.

Cooke DF, Stepniewska I, Miller DJ, Kaas JH, Krubitzer L. 2015. Reversible deactivation of motor cortex reveals functional connectivity with posterior parietal cortex in the prosimian galago (*Otolemur garnettii*). J Neurosci. 35:14406–14422.

Cooke DF, Taylor CS, Moore T, Graziano MS. 2003. Complex movements evoked by microstimulation of the ventral intraparietal area. Proc Natl Acad Sci USA. 100:6163–6168.

Coulter JD, Jones EG. 1977. Differential distribution of corticospinal projections from individual cytoarchitectonic fields in the monkey. Brain Res. 129:335–340.

Darling WG, Pizzimenti MA, Rotella DL, Hynes SM, Ge J, Stilwell-Morecraft K, Morecraft RJ. 2016. Sensorimotor cortex injury effects on recovery of contralesional dexterous movements in Macaca mulatta. Exp Neurol. 281:37–52.

Dea M, Hamadjida A, Elgbeili G, Quessy S, Dancause N. 2016. Different patterns of cortical inputs to subregions of the primary motor cortex hand representation in *Cebus apella*. Cereb Cortex. 26:1747–1761.

Debowy DJ, Ghosh S, Ro JY, Gardner EP. 2001. Comparison of neuronal firing rates in somatosensory and posterior parietal cortex during prehension. Exp Brain Res. 137:269–291.

De Villers-Sidani E, Chang EF, Bao S, Merzenich MM. 2007. Critical period window for spectral tuning defined in the primary auditory cortex (A1) in the rat. J Neurosci. 27(1): 180–189.

Dum RP, Strick PL. 2002. Motor areas in the frontal lobe of the primate. Physiol Behav. 77:677–682.

Downloaded from https://academic.oup.com/cercor/advance-article-abstract/doi/10.1093/cercor/bhx279/4608060
by University of California, Davis user
on 26 March 2018

Ferraina S, Bianchi L. 1994. Posterior parietal cortex: functional properties of neurons in area 5 during an instructed-delay reaching task within different parts of space. Exp Brain Res. 99:175–178.

Ferrier D. 1874. On the localisation of the functions of the brain. Br Med J. 2:766–767.

Fetz EE, Cheney PD. 1980. Postspike facilitation of forelimb muscle activity by primate corticomotoneuonal cells. J Neurophsiol. 44(4):751–72.

Flash T, Hochner B. 2005. Motor primitives in vertebrates and invertebrates. Curr Opin Neurobiol. 15:660–666.

Fleming JF, Crosby EC. 1955. The parietal lobe as an additional motor area; the motor effects of electrical stimulation and ablation of cortical areas 5 and 7 in monkeys. J Comp Neurol. 103:485–512.

Galea MP, Darian-Smith I. 1994. Multiple corticospinal neuron populations in the macaque monkey are specified by their unique cortical origins, spinal terminations, and connections. Cereb Cortex. 4:166–194.

Gallese V, Murata A, Kaseda M, Niki N, Sakata H. 1994. Deficit of hand preshaping after muscimol injection in monkey parietal cortex. Neuroreport. 5:1525–1529.

Gardner EP, Babu KS, Ghosh S, Sherwood A, Chen J. 2007a. Neurophysiology of prehension. III. Representation of object features in posterior parietal cortex of the macaque monkey. J Neurophysiol. 98:3708–3730.

Gardner EP, Babu KS, Reitzen SD, Ghosh S, Brown AS, Chen J, Hall AL, Herzlinger MD, Kohlenstein JB, Ro JY. 2007b. Neurophysiology of prehension. I. Posterior parietal cortex and object-oriented hand behaviors. J Neurophysiol. 97: 387–406.

Gharbawie OA, Stepniewska I, Burish MJ, Kaas JH. 2010. Thalamocortical connections of functional zones in posterior parietal cortex and frontal cortex motor regions in New World monkeys. Cereb Cortex. 20:2391–2410.

Gharbawie OA, Stepniewska I, Kaas JH. 2011a. Cortical connections of functional zones in posterior parietal cortex and frontal cortex motor regions in new world monkeys. Cereb Cortex. 21:1981–2002.

Gharbawie OA, Stepniewska I, Qi H, Kaas JH. 2011b. Multiple parietal-frontal pathways mediate grasping in macaque monkeys. J Neurosci. 31:11660–11677.

Godlove J, Gulati T, Dichter B, Chang E, Ganguly K. 2016. Muscle synergies after stroke are correlated with perilesional high gamma. Ann Clin Transl Neurol. 3:956–961.

Godschalk M, Mitz AR, van Duin B, van der Burg H. 1995. Somatotopy of monkey premotor cortex examined with microstimulation. Neurosci Res. 23:269–279.

Gould HJ 3rd, Cusick CG, Pons TP, Kaas JH. 1986. The relationship of corpus callosum connections to electrical stimulation maps of motor, supplementary motor, and the frontal eye fields in owl monkeys. J Comp Neurol. 247: 297–325.

Graziano MS. 2016. Ethological action maps: a paradigm shift for the motor cortex. Trends Cogn Sci. 20:121–132.

Graziano MS, Aflalo TN, Cooke DF. 2005. Arm movements evoked by electrical stimulation in the motor cortex of monkeys. J Neurophysiol. 94:4209–4223.

Graziano MS, Patel KT, Taylor CS. 2004. Mapping from motor cortex to biceps and triceps altered by elbow angle. J Neurophysiol. 92:395–407.

Graziano MS, Taylor CS, Moore T. 2002a. Complex movements evoked by microstimulation of precentral cortex. Neuron. 34:841–851.

Graziano MS, Taylor CS, Moore T, Cooke DF. 2002b. The cortical control of movement revisited. Neuron. 36:349–362.

Gregoriou GG, Borra E, Matelli M, Luppino G. 2006. Architectonic organization of the inferior parietal convexity of the macaque monkey. J Comp Neurol. 496:422–451.

Griffin DM, Hudson HM, Belhaj-Saif A, Cheney PD. 2011. Hijacking cortical motor output with repetitive microstimulation. J Neurosci. 31:13088–13096.

Griffin DM, Hudson HM, Belhaj-Saif A, Cheney PD. 2014. EMG activation patterns associated with high frequency, long-duration intracortical microstimulation of primary motor cortex. J Neurosci. 34:1647–1656.

Huntley GW, Jones EG. 1991. Relationship of intrinsic connections to forelimb movement representations in monkey motor cortex: a correlative anatomic and physiological study. J Neurophysiol. 66:390–413.

Jones EG, Coulter JD, Burton H, Porter R. 1977. Cells of origin and terminal distribution of corticostriatal fibers arising in the sensory-motor cortex of monkeys. J Comp Neurol. 173: 53–80.

Jones EG, Coulter JD, Hendry SH. 1978. Intracortical connectivity of architectonic fields in the somatic sensory, motor and parietal cortex of monkeys. J Comp Neurol. 181:291–347.

Kaas JH, Qi H, Stepniewska I. 2017. Evolution of parietal-frontal networks in primates. In: Kaas JH, Krubitzer LK, editors. Evolution of nervous systems. Elsavier. p. 287–297.

Kalaska JF. 1996. Parietal cortex area 5 and visuomotor behavior. Can J Physiol Pharmacol. 74:483–498.

Kambi N, Tandon S, Mohammed H, Lazar L, Jain N. 2011. Reorganization of the primary motor cortex of adult macaque monkeys after sensory loss resulting from partial spinal cord injuries. J Neurosci. 31:3696–3707.

Kasser RJ, Cheney PD. 1985. Characteristics of corticomotoneuronal postspike facilitation and reciprocal suppression of EMG activity in the monkey. J Neurophysiol. 53:959–978.

Keizer K, Kuypers HGJM. 1989. Distribution of corticospinal neurons with collaterals to the lower brain stem reticular formation in monkey (*Macaca fasciularis*). Exp Brain Res. 74: 311–318.

Kennard MA, Mc Culloch WS. 1943. Motor responses to stimulation of cerebral cortex in the absence of areas 4 and 6 (*Macaca mulatta*). J Neurophysiol. 6:181–189.

Kilgard MP, Merzenich MM. 1998. Cortical map reorganization enabled by nucleus basalis activity. Science. 279:1714–1718.

Krubitzer L, Huffman KJ, Disbrow E, Recanzone G. 2004. Organization of area 3a in macaque monkeys: contributions to the cortical phenotype. J Comp Neurol. 471:97–111.

Kwan HC, MacKay WA, Murphy JT, Wong YC. 1978. Spatial organization of precentral cortex in awake primates: II. Motor outputs. J Neurophysiol. 41:1120–1131.

Lacquaniti F, Guigon E, Bianchi L, Ferraina S, Caminiti R. 1995. Representing spatial information for limb movement: role of area 5 in the monkey. Cereb Cortex. 5:391–409.

Leyton ASF, Sherrington CS. 1917. Observations on the excitable cortex of the chimpanzee, orang-utan, and gorilla. Exp Physiol. 11:135–222.

Macfarlane NB, Graziano MS. 2009. Diversity of grip in *Macaca mulatta*. Exp Brain Res. 197:255–268.

Matelli M, Luppino G. 2001. Parietofrontal circuits for action and space perception in the macaque monkey. Neuroimage. 14: S27–32.

McGuinness E, Sivertsen D, Allman JM. 1980. Organization of the face representation in macaque motor cortex. J Comp Neurol. 193:591–608.

Downloaded from https://academic.oup.com/cercor/advance-article-abstract/doi/10.1093/cercor/bhx279/4608060
by University of California, Davis user
on 26 March 2018

Milliken GW, Plautz EJ, Nudo RJ. 2013. Distal forelimb representations in primary motor cortex are redistributed after forelimb restriction: a longitudinal study in adult squirrel monkeys. J Neurophysiol. 109:1268–1282.

Mountcastle VB, Lynch JC, Georgopoulos A, Sakata H, Acuna C. 1975. Posterior parietal association cortex of the monkey: command functions for operations within extrapersonal space. J Neurophysiol. 38:871–908.

Nelson RJ, Sur M, Felleman DJ, Kaas JH. 1980. Representations of the body surface in postcentral parietal cortex of *Macaca fascicularis*. J Comp Neurol. 192:611–643.

Nudo RJ, Masterton RB. 1990. Descending pathways to the spinal cord, III: Sites of origin of the corticospinal tract. J Comp Neurol. 296:559–583.

Nudo RJ, Jenkins WM, Merzenich MM, Prejean T, Grenda R. 1992. Neurophysiological correlates of hand preference in primary motor cortex of adult squirrel monkeys. J Neurosci. 12(8):2918–47.

Overduin SA, d'Avella A, Carmena JM, Bizzi E. 2012. Microstimulation activates a handful of muscle synergies. Neuron. 76:1071–1077.

Overduin SA, d'Avella A, Carmena JM, Bizzi E. 2014. Muscle synergies evoked by microstimulation are preferentially encoded during behavior. Front Comput Neurosci. 8:20.

Overduin SA, d'Avella A, Roh J, Carmena JM, Bizzi E. 2015. Representation of muscle synergies in the primate brain. J Neurosci. 35:12615–12624.

Padberg J, Cerkevich C, Engle J, Rajan AT, Recanzone G, Kaas J, Krubitzer L. 2009. Thalamocortical connections of parietal somatosensory cortical fields in macaque monkeys are highly divergent and convergent. Cereb Cortex. 19: 2038–2064.

Padberg J, Disbrow E, Krubitzer L. 2005. The organization and connections of anterior and posterior parietal cortex in titi monkeys: do New World monkeys have an area 2? Cereb Cortex. 15:1938–1963.

Penfield W, Boldrey E. 1937. Somatic motor and sensory reprsentation in the cerebral cortex of man as studied by electrical stimulation. Brain. 60:389–443.

Pons TP, Garraghty PE, Cusick CG, Kaas JH. 1985. The somatotopic organization of area 2 in macaque monkeys. J Comp Neurol. 241:445–466.

Pons TP, Kaas JH. 1986. Corticocortical connections of area 2 of somatosensory cortex in macaque monkeys: a correlative anatomical and electrophysiological study. J Comp Neurol. 248:313–335.

Preuss TM, Stepniewska I, Kaas JH. 1996. Movement representation in the dorsal and ventral premotor areas of owl monkeys: a microstimulation study. J Comp Neurol. 371: 649–676.

Qi HX, Jain N, Collins CE, Lyon DC, Kaas JH. 2010. Functional organization of motor cortex of adult macaque monkeys is altered by sensory loss in infancy. Proc Natl Acad Sci USA. 107:3192–31927.

Qi HX, Stepniewska I, Kaas JH. 2000. Reorganization of primary motor cortex in adult monkeys with long-standing amputations. J Neurophysiol. 84:2133–2147.

Rathelot JA, Dum RP, Strick PL. 2017. Posterior parietal cortex contains a command apparatus for hand movements. Proc Natl Acad Sci USA. 114:4255–4260.

Rathelot JA, Strick PL. 2006. Muscle representations in the macaque motor cortex: an anatomical perspective. Proc Natl Acad Sci USA. 103:8257–8262.

Rathelot JA, Strick PL. 2009. Subdivisions of primary motor cortex based on cortico-motoneuronal cells. Proc Natl Acad Sci USA. 106:918–923.

Remple MS, Reed JL, Stepneiwska I, Kaas JH. 2006. Orgnaization of frontal cortex in the tree shrew (*Tupaia belangeri*). I. Architecture, microelectrode maps, and corticopsinal connections. J Comp Neurol. 497:133–154.

Rouiller EM, Yu XH, Moret V, Tempini A, Wiesendanger M, Liang F. 1998. Dexterity in adult monkeys following early lesion of the motor cortical hand area: the role of cortex adjacent to the lesion. Eur J Neurosci. 10:729–740.

Rozzi S, Calzavara R, Belmalih A, Borra E, Gregoriou GG, Matelli M, Luppino G. 2006. Cortical connections of the inferior parietal cortical convexity of the macaque monkey. Cereb Cortex. 16:1389–1417.

Rozzi S, Ferrari PF, Bonini L, Rizzolatti G, Fogassi L. 2008. Functional organization of inferior parietal lobule convexity in the macaque monkey: electrophysiological characterization of motor, sensory and mirror responses and their correlation with cytoarchitectonic areas. Eur J Neurosci. 28: 1569–1588.

Sakata H, Taira M, Murata A, Mine S. 1995. Neural mechanisms of visual guidance of hand action in the parietal cortex of the monkey. Cereb Cortex. 5:429–438.

Schindelin J, Arganda-Carreras I, Frise E, Kaynig V, Longair M, Pietzsch T, Preibisch S, Rueden C, Saalfeld S, Schmid B, et al. 2012. Fiji: an open-source platform for biological-image analysis. Nat Methods. 9:676–682.

Seelke AM, Padberg JJ, Disbrow E, Purnell SM, Recanzone G, Krubitzer L. 2012. Topographic maps within Brodmann's area 5 of macaque monkeys. Cereb Cortex. 22:1834–1850.

Sessle BJ, Wiesendanger M. 1982. Structural and functional definition of the motor cortex in the monkey (*Macaca fascicularis*). J Physiol. 323:245–265.

Snyder LH, Batista AP, Andersen RA. 1997. Coding of intention in the posterior parietal cortex. Nature. 386:167–170.

Stepniewska I, Cerkevich CM, Fang PC, Kaas JH. 2009a. Organization of the posterior parietal cortex in galagos: II. Ipsilateral cortical connections of physiologically identified zones within anterior sensorimotor region. J Comp Neurol. 517:783–807.

Stepniewska I, Fang PC, Kaas JH. 2005. Microstimulation reveals specialized subregions for different complex movements in posterior parietal cortex of prosimian galagos. Proc Natl Sci USA. 102:4878–4883.

Stepniewska I, Fang PC, Kaas JH. 2009b. Organization of the posterior parietal cortex in galagos: I. Functional zones identified by microstimulation. J Comp Neurol. 517:765–782.

Stepniewska I, Friedman RM, Gharbawie OA, Cerkevich CM, Roe AW, Kaas JH. 2011. Optical imaging in galagos reveals parietal-frontal circuits underlying motor behavior. Proc Natl Acad Sci USA. 108:E725–732.

Stepniewska I, Gharbawie OA, Burish MJ, Kaas JH. 2014. Effects of muscimol inactivations of functional domains in motor, premotor, and posterior parietal cortex on complex movements evoked by electrical stimulation. J Neurophysiol. 111: 1100–1119.

Stepniewska I, Preuss TM, Kaas JH. 1993. Architectonics, somatotopic organization, and ipsilateral cortical connections of the primary motor area (M1) of owl monkeys. J Comp Neurol. 330:238–271.

Stoney SD Jr, Thompson WD, Asanuma H. 1968. Excitation of pyramidal tract cells by intracortical microstimulation:

Downloaded from https://academic.oup.com/cercor/advance-article-abstract/doi/10.1093/cercor/bhx279/4608060
by University of California, Davis user
on 26 March 2018

effective extent of stimulating current. J Neurophysiol. 31: 659–669.
Strick PL. 2002. Stimulating research on motor cortex. Nat Neurosci. 5:714–715.
Strick PL, Preston JB. 1982a. Two representations of the hand in area 4 of a primate. I. Motor output organizatino. J Neurophysiol. 48(1):139–49.
Taylor CS, Gross CG. 2003. Twitches versus movements: a story of motor cortex. Neuroscientist. 9:332–342.
Thier P, Andersen RA. 1998. Electrical microstimulation distinguishes distinct saccade-related areas in the posterior parietal cortex. J Neurophysiol. 80:1713–1735.
Toyoshima K, Sakai H. 1982. Exact cortical extent of the origin of the corticospinal tract (CST) and the quantitative contribution to the CST in different cytoarchitectonic areas. A study with horseradish peroxidase in the monkey. J Hirnforsch. 23:257–269.
Vassbo K, Nicotra G, Wiberg M, Bjaalie JG. 1999. Monkey somatosensory cerebrocerebellar pathways: uneven densities of corticopontine neurons in different body representations of areas 3b, 1, and 2. J Comp Neurol. 406: 109–128.
Vogt C, Vogt O. 1919. Allgemeinere Ergebnisse unserer Hirnforschung. J Psychol Neurol. 25:279–462.
Weinrich M, Wise SP. 1982. The premotor cortex of the monkey. J Neurosci. 2:1329–1345.
Widener GL, Cheney PD. 1997. Effects on muscle activity from microstimuli applied to somatosensory and motor cortex during voluntary movement in the monkey. J Neurophysiol. 77:2446–2465.
Wise SP, Boussaoud D, Johnson PB, Caminiti R. 1997. Premotor and parietal cortex: corticocortical connectivity and combinatorial computations. Annu Rev Neurosci. 20:25–42.
Woolsey CN, Travis AM, Barnard JW, Ostenso RS. 1953. Motor respresentation in the postcentral gyrus after chronic ablation of precentral and supplementary motor areas. Federation Proc. 12:160.
Wu CW, Bichot NP, Kaas JH. 2000. Converging evidence from microstimulation, architecture, and connections for multiple motor areas in the frontal and cingulate cortex of prosimian primates. J Comp Neurol. 423:140–177.
Yokochi H, Tanaka M, Kumashiro M, Iriki A. 2003. Inferior parietal somatosensory neurons coding face-hand coordination in Japanese macaques. Somatosens Mot Res. 20:115–125.

Downloaded from https://academic.oup.com/cercor/advance-article-abstract/doi/10.1093/cercor/bhx279/4608060
by University of California, Davis user
on 26 March 2018